

# VC-BART: Bayesian trees for varying coefficients

Sameer K. Deshpande\*, Ray Bai†, Cecilia Balocchi‡ and Jennifer E. Starling§

October 19, 2021

## Abstract

The linear varying coefficient (VC) model generalizes the conventional linear model by allowing the additive effect of each covariate on the outcome to vary as a function of additional effect modifiers. While there are many existing procedures for VC modeling with a single scalar effect modifier (often assumed to be time), there has, until recently, been comparatively less development for settings with multivariate modifiers. Unfortunately, existing state-of-the-art procedures that can accommodate multivariate modifiers typically make restrictive structural assumptions about the covariate effect functions or require intensive problem-specific hand-tuning that scales poorly to large datasets. In response, we propose VC-BART, which estimates the covariate effect functions in a VC model using Bayesian Additive Regression Trees (BART).

On several synthetic and real-world data sets, we demonstrate that, with simple default hyperparameter settings, VC-BART displays covariate effect recovery performance superior to state-of-the-art VC modeling techniques and predictive performance on par with more flexible but less interpretable nonparametric regression procedures. We further demonstrate the theoretical near-optimality of VC-BART by synthesizing recent theoretical results about the VC model and BART to derive posterior concentration rates in settings with independent and correlated errors. An R package implementing VC-BART is available at <https://github.com/skdeshpande91/VCBART>

---

\*Massachusetts Institute of Technology. [sameerd@alum.mit.edu](mailto:sameerd@alum.mit.edu)

†University of South Carolina

‡University of Pennsylvania

§The University of Texas at Austin

# 1 Introduction

Estimating the regression function  $\mathbb{E}[Y | W]$  is a natural first step towards uncovering important relationships between a vector of predictors  $W$  and a noisy outcome  $Y$ . It can feel as though we suffer from an embarrassment of riches when choosing a method with which to estimate the regression function. On the one hand, the barrier to deploy flexible methods like deep neural networks has never been lower. Such methods can produce extremely accurate and generalizable fits to complex data but are essentially blackboxes that are difficult to interpret and explain to our applied collaborators. On the other hand, there are inherently interpretable techniques like the workhorse generalized linear model. Unfortunately, interpretability often comes at the cost of model flexibility in the form of strong assumptions about the relationships between  $W$  and  $Y$ . A growing need and desire for flexible-yet-interpretable models has recently sparked tremendous activity within the statistics and machine learning community (Doshi-Velez and Kim, 2017; Murdoch et al., 2019). It is in milieu that we revisit the linear varying coefficient (VC) model.

VC modeling begins by splitting the components of  $W$  into two (possibly overlapping) groups: a set of  $p$  *covariates*, which we denote by  $X$ , and a set of  $R$  *effect modifiers*, which we denote by  $Z$ . We then model

$$Y = \beta_0(Z) + \beta_1(Z)X_1 + \dots + \beta_p(Z)X_p + \varepsilon \tag{1}$$

where the  $\beta_0(Z), \dots, \beta_p(Z)$  are *functions* mapping  $\mathbb{R}^R$  to  $\mathbb{R}$  and the residual error  $\varepsilon$  has mean zero. At first glance, the model in (1) appears to be a typographical extension of the conventional linear model. However, many well-known semi-parametric and nonparametric models arise as special cases of the general linear VC model, including partially linear models (Härdle et al., 2000) and generalized additive models (Hastie and Tibshirani, 1986). Since its introduction in Hastie and Tibshirani (1993), the VC model has proven quite popular, offering a compelling balance between model flexibility and interpretability.

Until recently, the vast majority of the VC literature focused on settings with only a single effect modifier, often assumed to be time. We increasingly face situations in which the covariate effects might vary with respect to multiple effect modifiers. For instance, in one of our illustrative examples we investigate how the effect of an additional year of education on earnings varies with respect to gender, race, and labor market experience. Later, we study spatiotemporal variability in the effect of income on urban crime levels.

Many state-of-the-art methods for modeling with multivariate modifiers unfortunately impose rigid additive assumptions about the functional form of the  $\beta_j$ 's and require computationally intensive tuning. Further, nearly all of the default implementations of these procedures do not provide any uncertainty quantification about estimated covariate effects  $\beta_j(Z)$  or a new predictions  $y^*$ .

In sharp contrast to existing methods, we present **VC-BART**, a Bayesian nonparametric approach for fitting the model in (1). VC-BART, an extension of [Chipman et al. \(2010\)](#)'s Bayesian Additive Regression Trees (BART) model, approximates each covariate effect function  $\beta_j(Z)$  as a sum of shallow piecewise constant regression trees. On several synthetic and real-world examples, we demonstrate that *without requiring intensive hand-tuning or imposing strong structural assumptions*, VC-BART exhibits superior covariate effect estimation compared to the current state-of-the-art. Additionally, VC-BART automatically quantifies uncertainty in a coherent and generally well-calibrated fashion. We moreover find that compared to more flexible blackbox procedures, VC-BART can provide substantially more interpretable fits to data without sacrificing predictive power. We synthesize recent theoretical results about BART and the general VC model to show that under mild conditions, the VC-BART posterior concentrates at a *near-optimal* rate when the residual errors  $\varepsilon$  in Equation (1) are independent (Theorem 1) and when the residuals errors are correlated (Theorem 2). To the best of our knowledge, Theorem 2 is the first result to demonstrate the theoretical near-optimality of Bayesian treed regression in settings with non-i.i.d. noise.

Here is an outline for the rest of paper. We review relevant background on BART and varying coefficient modeling in Section 2. In Section 3, we introduce VC-BART and describe how to perform posterior inference using Bayesian backfitting ([Hastie and Tibshirani, 2000](#)). We state our asymptotic results in Section 4. In Section 5, we examine VC-BART's covariate effect recovery and predictive capabilities with several synthetic experiments. We illustrate the use of VC-BART with two real-world applications: an analysis of returns to education and a spatiotemporal analysis of crime in Philadelphia in Section 6. We conclude with a discussion and outline several avenues of future work in Section 7.

## 2 Background

### 2.1 Varying Coefficient Models

In this paper, we study two types of VC models, a “cross-sectional” model with independent observations and a “panel” model for repeated observations. After presenting both models, we briefly review relevant VC literature.

**Cross-sectional model.** We first consider the cross-sectional model in which we have  $n$  independent observations of (i) a scalar outcome  $y \in \mathbb{R}$ , (ii) a  $p$ -dimensional vector of covariates  $\mathbf{x} = (x_1, \dots, x_p)$ , and (iii) an  $R$ -dimensional vector of effect modifiers  $\mathbf{z} = (z_{i1}, \dots, z_{iR})$ . We model

$$y_i = \beta_0(\mathbf{z}_i) + \sum_{j=1}^p \beta_j(\mathbf{z}_i)x_{ij} + \sigma\varepsilon_i; \quad \varepsilon_i \stackrel{\text{i.i.d.}}{\sim} \mathcal{N}(0, 1) \quad (2)$$

In Section 6.1, we use this cross-sectional model to study the returns to education.

**Panel model.** We also consider a panel model in which we repeatedly observe  $n$  independent subjects over time. Specifically for each subject  $i = 1, \dots, n$ , we observe triplets  $(\mathbf{x}_{it}, \mathbf{z}_{it}, y_{it})$  of covariates, modifiers, and outcomes at  $n_i$  time points  $t = t_{i1}, \dots, t_{in_i}$ . For all  $i = 1, \dots, n$ , and  $t = 1, \dots, n_i$ , we model

$$y_{it} = \beta_0(\mathbf{z}_{it}) + \sum_{j=1}^p \beta_j(\mathbf{z}_{it})x_{itj} + \sigma\varepsilon_{it}. \quad (3)$$

In the panel setting, we assume that the subject-specific noise vectors  $\boldsymbol{\varepsilon}_i = (\varepsilon_{i1}, \dots, \varepsilon_{in_i})^\top \sim \mathcal{N}_{n_i}(\mathbf{0}_{n_i}, \boldsymbol{\Sigma}_i(\rho))$  are independent across subjects. Like Bai et al. (2019a), we focus on the class of correlation matrices  $\boldsymbol{\Sigma}_i(\rho)$  whose entries are parametrized with a single autocorrelation parameter  $\rho \in [0, 1]$ . This class includes many popular correlation structures, including the first-order autoregressive model in which the  $(j, k)$  element of  $\boldsymbol{\Sigma}(\rho)$  is  $\rho^{|t_{ij} - t_{ik}|}$  and the compound symmetry model where all off-diagonal elements of  $\boldsymbol{\Sigma}(\rho)$  are equal to  $\rho$ . In Section 6.2, we study the spatiotemporal variation of urban crime with a panel VC model.

**Relevant literature.** Since their introduction in Hastie and Tibshirani (1993), VC models have been extensively studied in both the statistics and econometrics literature. We give a brief overview of this literature and refer the reader to Fan and Zhang (2008), Park et al. (2015), and Franco-Villoria et al. (2019) for more comprehensive reviews. When there is

only a single modifier (i.e.  $R = 1$ ), one popular approach (see, e.g., Hoover et al. (1998) and Huang et al. (2002)) is to express each  $\beta_j$  as a linear combination of  $q_j$  pre-specified basis functions. Such a decomposition effectively reduces the functional regression problem to high-dimensional linear regression problem for which numerous frequentist (see, e.g. Wang et al., 2008; Wang and Xia, 2009; Wei et al., 2011) and Bayesian (Bai et al., 2019a) regularization techniques have been proposed. Kernel smoothing is another popular and theoretically supported alternative (see, e.g., Wu and Chiang, 2000).

In the multivariate modifier setting, Tibshirani and Friedman (2019) and Lee et al. (2018) respectively constrain the  $\beta_j$ 's to be linear and additive functions of the components of  $\mathbf{z}$ . In contrast, Li and Racine (2010) propose a multivariate kernel smoothing estimator that imposes no rigid structural assumptions on the  $\beta_j$ 's. Unfortunately, their estimator requires tuning several bandwidth parameters with leave-one-out cross-validation. When any of  $n, p$  and  $R$  are large, this becomes computationally prohibitive.

In the last decade or so, several authors have approximated the  $\beta_j(\mathbf{z})$ 's with ensembles of regression trees. Wang and Hastie (2012) and Zhou and Hooker (2019) both use boosting to construct separate ensembles for each  $\beta_j$ . While trees are an intuitively appealing and readily scalable approach to multiple modifiers, their procedures require substantial tuning to set the learning rate and number of boosting iterations. To the best of our knowledge, no existing procedure for VC modeling with multivariate modifiers provides any non-asymptotic uncertainty quantification.

## 2.2 Bayesian Additive Regression Trees

We now briefly describe BART. To set our notation, let  $T$  denote a binary decision tree partitioning  $\mathbb{R}^R$  that consists of a collection of interior nodes and  $L(T)$  terminal or *leaf* nodes. We associate an axis-aligned decision rule of the form  $\{Z_v < c\}$  or  $\{Z_v \geq c\}$  to each internal (i.e. non-leaf) node of  $T$ . These decision rules are uniquely determined by the pair  $(v, c)$  of variable index  $v$  and cut-point  $c$ . The  $L(T)$  leaves of  $T$  partition  $\mathbb{R}^R$  into rectangular cells and we let  $\ell(\mathbf{z}; T)$  be the function that returns the index of the leaf containing the point  $\mathbf{z}$ . A *regression tree* is a pair  $(T, \boldsymbol{\mu})$  consisting of a decision tree  $T$  and collection of *jumps*  $\boldsymbol{\mu} = \{\mu_1, \dots, \mu_{L(T)}\}$  associated with each leaf of  $T$ . The evaluation function  $g(\mathbf{z}; T, \boldsymbol{\mu}) = \mu_{\ell(\mathbf{z}; T)}$  returns the jump corresponding to the leaf containing  $\mathbf{z}$ .

In the standard univariate non-parameter regression problem  $y = f(\mathbf{z}) + \sigma\varepsilon; \quad \varepsilon \sim N(0, 1)$ ,

Chipman et al. (2010) approximated the unknown regression function  $f$  with a sum of  $M$  regression trees

$$f(\mathbf{z}) \approx \sum_{m=1}^M g(\mathbf{z}; T_m, \boldsymbol{\mu}_m),$$

which were each given independent priors. Priors over the regression trees  $(T_m, \boldsymbol{\mu}_m)$  were then updated to compute an approximate posterior over  $f$ . Chipman et al. (2010) specify the regression tree prior in two parts, a prior over the decision tree  $T$  and a conditional prior over the jumps  $\boldsymbol{\mu} \mid T$ . They used a branching process prior for  $T$ , which can be described by three aspects: (i) the probability that a node at depth  $d$  is non-terminal, which is given by  $\alpha(1+d)^{-\beta}$ , (ii) a uniform distribution on the splitting variable index  $v$  associated to each non-terminal node, and (iii) a uniform distribution on the cut-points  $c$  at each non-terminal node. Conditional on the tree  $T$ , jumps in  $\boldsymbol{\mu}$  were given independent  $\mathcal{N}(0, \tau^2)$  priors.

In all, the BART prior depends on several hyperparameters: the number of trees  $M$ , the parameters of the latent branching process  $\alpha$  and  $\beta$ , and the prior standard deviation  $\tau$  of jumps. Chipman et al. (2010) demonstrated that there is a *default* set of hyper-parameters that works remarkably well across a wide variety of problems. In particular, they recommended fixing  $\alpha = 0.95$  and  $\beta = 2$  so that the prior places overwhelming probability on trees with depth five or less. Noting that the  $\mathcal{N}(0, \tau^2)$  prior on the jumps  $\boldsymbol{\mu}$  implies  $f(\mathbf{z}) \sim \mathcal{N}(0, M\tau^2)$ , they recommend setting  $\tau$  so that the marginal prior of  $f(\mathbf{z})$  places substantial probability over the range of the observed data.

The basic BART model has been extended successfully to survival analysis (Sparapani et al., 2016), multiple imputation (Xu et al., 2016), log-linear models for multinomial and count data (Murray, 2019), semi-continuous responses (Linero et al., 2019), and causal inference (Hill, 2011; Hahn et al., 2020; Sivaganesan et al., 2017; Logan et al., 2019). BART has also been modified to recover smooth (Linero and Yang, 2018; Starling et al., 2019b) and monotonic (Chipman et al., 2019; Starling et al., 2019a) functions. In each of these settings, new BART-based methods often substantially outperform existing state-of-the-art procedures in terms of function recovery and prediction. Moreover, recent results in Ročková and van der Pas (2019) and Ročková and Saha (2019) demonstrate BART’s theoretical near-optimality under very mild assumptions. We refer the reader to Tan and Roy (2019) for a more detailed review of BART and its many extensions.

### 3 The VC–BART Procedure

The key idea of our proposed procedure, VC-BART, is to place independent BART priors on each of the covariate effect functions in (1). In other words, we introduce  $p + 1$  collections of  $M$  regression trees  $\mathcal{E}_j = \{(T_m^{(j)}, \boldsymbol{\mu}_m^{(j)})\}_{m=1}^M$ , one for each  $\beta_j$ , and approximate

$$\beta_j(\mathbf{z}) \approx \sum_{m=1}^M g(\mathbf{z}; T_m^{(j)}, \boldsymbol{\mu}_m^{(j)}).$$

Because the resulting posterior distribution over regression trees is analytically intractable, we use a Markov Chain Monte Carlo (MCMC) simulation to draw posterior samples. In the next two subsections, we describe our posterior sampling strategy in both the cross-sectional and panel data settings. Throughout, we assume that the outcome and covariates have been centered and scaled to have mean zero and variance one and we will let  $\boldsymbol{\mathcal{E}}$  denote the full collection  $\{\mathcal{E}_0, \dots, \mathcal{E}_p\}$  of  $M(p + 1)$  regression trees.

#### 3.1 The cross-sectional VC-BART posterior

We place identical priors over each of the  $M(p + 1)$  trees in  $\boldsymbol{\mathcal{E}}$  and use [Chipman et al. \(2010\)](#)'s branching process prior on the decision trees  $T_m^{(j)}$ : the probability that a node at depth  $d$  is non-terminal is  $0.95(1 + d)^{-2}$  and we uniformly sample the splitting variable index and cut-point associated to each non-terminal node. We complete our prior specification with a half- $t$  prior on  $\sigma$  with density  $\pi(\sigma) \propto (\nu + \sigma^2)^{-\frac{1+\nu}{2}}$ . For simplicity, we take  $\nu = 7$ ,  $M = 50$  and set  $\tau_j = M^{-\frac{1}{2}}$  for each  $j$ . While this simple choice is decidedly arbitrary, we have found that it works quite well in practice, on both real and synthetic data.

Under the cross-sectional linear VC model of (2), the joint posterior density of the full tree ensemble  $\boldsymbol{\mathcal{E}}$  and residual standard deviation  $\sigma$  is given by

$$\pi(\boldsymbol{\mathcal{E}}, \sigma \mid \mathbf{Y}) \propto \sigma^{-n} (\nu + \sigma^2)^{-\frac{\nu+1}{2}} \exp \left\{ -\frac{\|\mathbf{R}\|_2^2}{2\sigma^2} \right\} \times \prod_{j=0}^p \prod_{m=1}^M \pi(T_m^{(j)}) \tau_j^{-L_m^{(j)}} \exp \left\{ -\frac{\|\boldsymbol{\mu}_m^{(j)}\|_2^2}{2\tau_j^2} \right\}, \quad (4)$$

where  $L_m^{(j)}$  is the number of leaves in tree  $T_m^{(j)}$  and  $\mathbf{R} = (R_1, \dots, R_n)^\top$  is the vector of *full*

residuals

$$R_i = y_i - \sum_{m=1}^M g(\mathbf{z}_i; T_m^{(0)}, \boldsymbol{\mu}_m^{(0)}) - \sum_{j=1}^p \sum_{m=1}^M x_{ij} g(\mathbf{z}_i; T_m^{(j)}, \boldsymbol{\mu}_m^{(j)}).$$

We use a Metropolis–within–Gibbs sampler to simulate draws from the posterior distribution of  $(\boldsymbol{\mathcal{E}}, \sigma)$ . At a high level, our sampler iterates between two steps: (i) sequentially updating each tree in  $\boldsymbol{\mathcal{E}}$  one at a time and (ii) updating  $\sigma^2$  conditionally on  $\boldsymbol{\mathcal{E}}$ .

**Updating a single tree.** To describe the Gibbs update of a single regression tree, we require some additional notation. First, for an arbitrary decision tree  $T$  with  $L$  leaves, let  $X(T)$  be the  $n \times L$  matrix whose  $(i, \ell)$  entry is equal to  $x_{ij}$  if observation  $i$  is associated with leaf  $\ell$  in  $T$  and is zero otherwise.

Now, suppose we are updating the  $m^{\text{th}}$  regression tree  $(T_m^{(j)}, \boldsymbol{\mu}_m^{(j)})$  in the ensemble  $\mathcal{E}_j$  used to approximate  $\beta_j$ . Let  $\boldsymbol{\mathcal{E}}^-$  denote the collection of all remaining  $M(p+1) - 1$  regression trees, where, for notational compactness, we have suppressed the dependence of this collection on the indices  $j$  and  $m$ . Additionally, let  $\mathbf{r} = (r_1, \dots, r_n)^\top$  be the vector of *partial residuals*  $r_i = R_i + x_{ij}g(\mathbf{z}_i; T_m^{(j)}, \boldsymbol{\mu}_m^{(j)})$ , where we have again suppressed the dependence on  $j$  and  $m$ . With our new notation, we immediately compute  $\mathbf{R} = \mathbf{r} - X(T_m^{(j)})\boldsymbol{\mu}_m^{(j)}$ .

It turns out the conditional posterior distribution of  $(T_m^{(j)}, \boldsymbol{\mu}_m^{(j)})$  depends on  $\mathbf{Y}$ ,  $\boldsymbol{\mathcal{E}}^-$ , and  $\sigma$  only through the partial residuals  $\mathbf{r}$ . In fact, using calculations reminiscent of conjugate Bayesian linear regression, we can decompose the conditional posterior density  $\pi(T, \boldsymbol{\mu} \mid \mathbf{Y}, \boldsymbol{\mathcal{E}}^-, \sigma)$  as

$$\pi(T \mid \mathbf{Y}, \boldsymbol{\mathcal{E}}^-, \sigma) \propto \tau_j^{-L(T)} |\Lambda(T)|^{\frac{1}{2}} \pi(T) \exp \left\{ \frac{1}{2} \Theta(T)^\top \Lambda(T) \Theta(T) \right\} \quad (5)$$

$$\pi(\boldsymbol{\mu} \mid T, \mathbf{Y}, \boldsymbol{\mathcal{E}}^-, \sigma) \propto |\Lambda(T)|^{-\frac{1}{2}} \exp \left\{ -\frac{1}{2} (\boldsymbol{\mu} - \Lambda(T)\Theta(T))^\top \Lambda(T)^{-1} (\boldsymbol{\mu} - \Lambda(T)\Theta(T)) \right\} \quad (6)$$

where  $\Lambda(T) = [\tau_j^{-2} I_{L(T)} + \sigma^{-2} X(T)^\top X(T)]^{-1}$  and  $\Theta(T) = \sigma^{-2} X(T)^\top \mathbf{r}$ .

Armed with these two conditional densities, we proceed exactly like [Chipman et al. \(2010\)](#): we draw a new decision tree  $T^*$  from a distribution with mass function (5) using a Metropolis–Hastings (MH) step and then, conditionally on  $T^*$ , we draw the new jumps  $\boldsymbol{\mu}$  from a  $N(\Lambda(T^*)\Theta(T^*), \Lambda(T^*))$  distribution. In our MH step, we construct the proposal tree  $T^*$  from the current tree  $T_m^{(j)}$  by either splitting a uniformly selected leaf node into two children or collapsing a uniformly selected pair of adjacent leaf nodes back to their common parent. We propose each type of transition with equal probability.



**Updating  $\sigma$ .** After updating each tree in  $\mathcal{E}$ , we draw a new value of  $\sigma$  conditionally on  $\mathbf{Y}$  and  $\mathcal{E}$  with another MH step. In this step, we use a transition density that is equal to the conditional posterior density of  $\sigma$  that we would have obtained had we initially specified a non-informative Jeffrey’s prior on  $\sigma$ . This choice of transition density, which [Linero and Yang \(2018\)](#) also use, facilitates considerable cancellation in computing the MH acceptance probability; see Section [S1](#) in the Supplementary Materials for further details.

### 3.2 The panel VC-BART posterior

In the panel data setting, we use the exact same prior choices for the  $\beta_j$ ’s and  $\sigma$  as in the cross-sectional setting. We additionally place a uniform prior on the autocorrelation parameter  $\rho$ . The joint posterior density of  $(\mathcal{E}, \sigma, \rho)$  is given by

$$\begin{aligned} \pi(\mathcal{E}, \sigma, \rho \mid \mathbf{Y}) &\propto (\nu + \sigma^2)^{-\frac{\nu+1}{2}} \times \prod_{i=1}^n \sigma^{-n_i} |\boldsymbol{\Omega}_i(\rho)|^{\frac{1}{2}} \exp \left\{ -\frac{\mathbf{R}_i^\top \boldsymbol{\Omega}_i(\rho) \mathbf{R}_i}{2\sigma^2} \right\} \\ &\times \prod_{j=0}^p \prod_{m=1}^M \pi(T_m^{(j)}) \tau_j^{-L_m^{(j)}} \exp \left\{ -\frac{\|\mu_m^{(j)}\|_2^2}{2\tau_j^2} \right\}, \end{aligned} \tag{7}$$

where  $\boldsymbol{\Omega}_i(\rho) = \boldsymbol{\Sigma}_i^{-1}(\rho)$  and the vector of subject  $i$ ’s full residuals  $\mathbf{R}_i = (R_{i1}, \dots, R_{in_i})^\top$  is defined similarly to full residuals  $\mathbf{R}$  in the cross-sectional setting.

It is straightforward to extend the cross-sectional Gibbs sampler to sample from  $\pi(\mathcal{E}, \sigma \mid \mathbf{Y}, \rho)$  for a fixed autocorrelation parameter  $\rho$ . While it is tempting to sample  $\rho$  conditionally on  $\mathbf{Y}$ ,  $\mathcal{E}$  and  $\sigma$ , we have found that the conditional posterior  $\pi(\rho \mid \mathcal{E}, \sigma, \mathbf{Y})$  tends to be extremely concentrated around the current value of  $\rho$ , resulting in slow mixing. As a result, like [Hoover et al. \(1998\)](#), we do not attempt to model the specific correlation structure of the  $\varepsilon_{it}$ ’s in [\(3\)](#) jointly with  $\mathcal{E}$  and  $\sigma$ . In fact, our simulation studies in Section [5.2](#) suggest that our that our point estimates of  $\beta_j(\mathbf{z})$  and out-of-sample predictions are often insensitive to potential misspecification of  $\rho$ .

## 4 Asymptotic Theory

VC-BART produces a posterior distribution over the function values  $\beta_j(\mathbf{z})$ . In this section, we answer the following question: as we observe more and more data generated from [\(1\)](#),

how quickly does the VC-BART posterior collapse to the true function values?

As noted in Ghosal et al. (2000), no posterior over the  $\beta_j(\mathbf{z})$ 's can contract faster than the minimax estimation rate. Theorems 1 and 2 show that in both the cross-sectional and panel data settings, the VC-BART posterior concentrates at a *near*-optimal rate that differs from the minimax rate by only a logarithmic factor.

We use the following notation in this section. For two nonnegative sequences  $\{a_n\}$  and  $\{b_n\}$ , we write  $a_n \asymp b_n$  to denote  $0 < \liminf_{n \rightarrow \infty} a_n/b_n \leq \limsup_{n \rightarrow \infty} a_n/b_n < \infty$ . If  $\lim_{n \rightarrow \infty} a_n/b_n = 0$ , we write  $a_n = o(b_n)$  or  $a_n \prec b_n$ . We use  $a_n \lesssim b_n$  or  $a_n = O(b_n)$  to denote that for sufficiently large  $n$ , there exists a constant  $C > 0$  independent of  $n$  such that  $a_n \leq Cb_n$ . For a function  $\beta$ ,  $\|\beta\|_\infty = \max_{\mathbf{z} \in \mathbb{R}^R} |\beta(\mathbf{z})|$ . Finally, for a symmetric matrix  $\mathbf{A}$ , we let  $\lambda_{\min}(\mathbf{A})$  and  $\lambda_{\max}(\mathbf{A})$  denote its minimum and maximum eigenvalues.

## 4.1 Cross-Sectional Model

Assume that there are true functions  $\beta_{0,0}, \dots, \beta_{0,p}$  such that

$$y_i = \beta_{0,0}(\mathbf{z}_i) + \sum_{j=1}^p \beta_{0,j}(\mathbf{z}_i)x_{ij} + \sigma_0\varepsilon_i, \quad i = 1, \dots, n, \quad (8)$$

where  $\varepsilon_i \sim \mathcal{N}(0, 1)$ ,  $\sigma_0 > 0$ . Let  $\boldsymbol{\beta}$  and  $\boldsymbol{\beta}_0$  be  $n \times (p+1)$  matrices whose respective  $(i, j)$  entries are  $\beta_j(\mathbf{z}_i)$  and  $\beta_{0,j}(\mathbf{z}_i)$ . We derive the posterior contraction rate with respect to the empirical  $\ell_2$  norm

$$\|\boldsymbol{\beta} - \boldsymbol{\beta}_0\|_n^2 = n^{-1} \sum_{i=1}^n \sum_{j=0}^p [\beta_j(\mathbf{z}_i) - \beta_{0,j}(\mathbf{z}_i)]^2.$$

To facilitate our theoretical analysis, like Ročková and Saha (2019), we modify the branching process prior on the decision tree  $T$  so that its splitting probability decays exponentially with depth rather than polynomially. We additionally assume the following regularity conditions:

- (A1)  $\beta_{0,j}$  is  $\alpha_j$ -Hölder continuous with  $0 < \alpha_j \leq 1$  and  $\|\beta_{0,j}\|_\infty \lesssim (\log n)^{1/2}$  for  $0 \leq j \leq p$
- (A2) There exists  $D_1 > 0$  so that  $|x_{ij}| \leq D_1$  for all  $1 \leq i \leq n, 1 \leq j \leq p$ .
- (A3)  $p = o(n^{2\alpha_m/(2\alpha_{\min}+R)})$  and  $R = O((\log n)^{1/2})$ , where  $\alpha_{\min} = \min\{\alpha_0, \dots, \alpha_p\}$ .

Assumption (A1) restricts the true  $\beta_{0,j}$ 's to be continuous with Hölder exponents less than

or equal to one. As noted in Ročková and van der Pas (2019), this restriction is essentially necessary since BART uses step functions to estimate  $\beta_0$ . Assumption (A2) requires that the covariates are uniformly bounded. Finally, Assumption (A3) allows the number of covariates  $p$  to diverge to infinity but at a slower rate than  $n$ . This assumption is needed to ensure that the contraction rate converges to zero as  $n, p \rightarrow \infty$ . The high-dimensional scenario where  $p \gg n$  and  $\beta_0$  is potentially sparse will be addressed in future work. Assumption (A3) also allows the number of effect modifiers  $R$  to grow with  $n$ , but at a much slower rate.

If we knew the true smoothness level  $\alpha_j$  of each  $\beta_j$ , the minimax-optimal rate for estimating  $\beta_0$  would be  $r_n^2 = \sum_{j=0}^p n^{-2\alpha_j/(2\alpha_j+R)}$  (Ročková and van der Pas, 2019). In the absence of such oracle information, our first result shows that we can estimate  $\beta_0$  at nearly this rate, sacrificing only a logarithmic factor.

**Theorem 1.** *Under (8), suppose we endow  $(\beta, \sigma)$  with a VC-BART prior, where the splitting probability of each node at depth  $d$  in a decision tree is given by  $\gamma^d$ , for some  $n^{-1} \leq \gamma < 0.5$ , and  $\nu > 1$  in the prior on  $\sigma$ . Assume that (A1)-(A3) hold. Then, for some constant  $M_1 > 0$  and  $r_n^2 = \log n \sum_{j=0}^p n^{-2\alpha_j/(2\alpha_j+R)}$ ,*

$$\Pi(\beta : \|\beta - \beta_0\|_n > M_1 r_n | \mathbf{Y}) \rightarrow 0, \quad (9)$$

in  $\mathbb{P}_{\beta_0}^{(n)}$ -probability as  $n, p \rightarrow \infty$ .

The proof of Theorem 1 is given in Section S2 of the Supplementary Materials and is based on first principles for verifying prior concentration and testing conditions.

## 4.2 Panel Model

In panel setting, we assume that the true model is

$$y_{it} = \beta_{0,0}(\mathbf{z}_{it}) + \sum_{j=0}^p \beta_{0,j}(\mathbf{z}_{it}) x_{itj} + \sigma_0 \varepsilon_{it}, \quad i = 1, \dots, n, t = 1, \dots, n_i, \quad (10)$$

where  $\varepsilon_i = (\varepsilon_{i1}, \dots, \varepsilon_{in_i})^\top \sim \mathcal{N}(\mathbf{0}_{n_i}, \Sigma_i(\rho_0))$ .

Let  $N = \sum_{i=1}^n n_i$  be the total number of observations across all  $n$  subjects and let  $n_{\max} =$

$\max\{n_1, \dots, n_n\}$ . We study the contraction rate of the VC-BART posterior under the norm

$$\|\boldsymbol{\beta} - \boldsymbol{\beta}_0\|_N^2 = N^{-1} \sum_{i=i}^n \sum_{t=1}^{n_i} \sum_{j=0}^p [\beta_j(\mathbf{z}_{it}) - \beta_{0,j}(\mathbf{z}_{it})]^2,$$

where the  $N \times (p+1)$  matrices  $\boldsymbol{\beta}$  and  $\boldsymbol{\beta}_0$  are defined similarly as above.

We assume the following regularity conditions:

(B1)  $\beta_{0,j}$  is  $\alpha_j$ -Hölder continuous with  $0 < \alpha_j \leq 1$  and  $\|\beta_{0,j}\|_\infty \lesssim (\log N)^{1/2}$  for  $0 \leq j \leq p$

(B2) There exists  $D_2 > 0$  so that  $|x_{itj}| \leq D_2$  for all  $1 \leq i \leq n, 1 \leq t \leq n_i, 1 \leq j \leq p$ .

(B3)  $p = o(N^{2\alpha_{\min}/(2\alpha_{\min}+R)})$ ,  $R = O((\log N)^{1/2})$ , and  $n_{\max} \asymp N/n$ .

(B4) The eigenvalues of each within-subject correlation matrix  $\boldsymbol{\Sigma}_i$  satisfy

$$1 \lesssim \min_{1 \leq i \leq n} \lambda_{\min}(\boldsymbol{\Sigma}_i(\rho_0)) \leq \max_{1 \leq i \leq n} \lambda_{\max}(\boldsymbol{\Sigma}_i(\rho_0)) \lesssim 1,$$

and for any  $(\sigma_1^2, \rho_1), (\sigma_2^2, \rho_2) \in (0, \infty) \times (0, 1)$

$$\begin{aligned} \max_{1 \leq i \leq n} \|\sigma_1^2 \boldsymbol{\Sigma}_i(\rho_1) - \sigma_2^2 \boldsymbol{\Sigma}_i(\rho_2)\|_F^2 &\leq \frac{1}{n} \|\sigma_1^2 \boldsymbol{\Sigma}(\rho_1) - \sigma_2^2 \boldsymbol{\Sigma}(\rho_2)\|_F^2 \\ &\lesssim n_{\max}^2 (\sigma_1^2 - \sigma_2^2)^2 + n_{\max}^4 \sigma_2^2 |\rho_1 - \rho_2|^2. \end{aligned}$$

where  $\boldsymbol{\Sigma} = \text{diag}(\boldsymbol{\Sigma}_1, \dots, \boldsymbol{\Sigma}_n)$ .

Assumptions (B1)-(B3) are essentially analogs of assumptions (A1)-(A3). Assumption (B4) assumes that the within-subject correlation matrices are asymptotically well-behaved in the sense that the eigenvalues for every  $\boldsymbol{\Sigma}_i$  are bounded away from zero and infinity, and the maximum squared Frobenius norm for the difference between any two correlation matrices of size  $n_i \times n_i$  is bounded above by a function of  $n_{\max}$ . These assumptions were also used in [Bai et al. \(2019a\)](#) and, as noted in that work, hold for several correlation structures, including first-order autoregressive, compound symmetry, and moving average. Under the true panel model (10), the VC-BART posterior also contracts at the near-optimal rate.

**Theorem 2.** *Under (10), suppose we endow  $(\boldsymbol{\beta}, \sigma)$  with a VC-BART prior, where the splitting probability of each node at depth  $d$  in a decision tree is given by  $\gamma^d$ , for some  $N^{-1} \leq \gamma < 0.5$ , and  $\nu > 1$  in the prior on  $\sigma$ . Suppose we further endow  $\rho$  with the uniform prior,  $\rho \sim \mathcal{U}(0, 1)$ . Assume that (B1)-(B4) hold. Then for some constant  $M_2 > 0$  and*

$$r_N^2 = \log N \sum_{j=0}^p N^{-2\alpha_j/(2\alpha_j+R)},$$

$$\Pi(\boldsymbol{\beta} : \|\boldsymbol{\beta} - \boldsymbol{\beta}_0\|_N > M_2 r_N | \mathbf{Y}) \rightarrow 0, \quad (11)$$

in  $\mathbb{P}_{\boldsymbol{\beta}_0}^{(N)}$ -probability as  $n, p \rightarrow \infty$ .

The proof of Theorem 2 is in Section S2 of the Supplementary Materials.

## 5 Synthetic Experiments

In this section, we demonstrate the application of VC-BART on several synthetic examples. In Section 5.1, we compare VC-BART’s ability to recover the covariate effect functions  $\beta_j(\mathbf{z})$  in the cross-sectional setting to two state-of-the-art VC methods. We continue with a comparison of the predictive performance of VC-BART and several blackbox procedures. We then consider the panel model in Section 5.2 and investigate VC-BART’s sensitivity to potential misspecification of the within-subject error correlation structure.

Throughout these experiments, we run two independent chains of VC-BART for 1,250 iterations, discarding the first 250 samples of each as burn-in. We approximate each  $\beta_j$  with an ensemble of  $M = 50$  trees and set each  $\tau_j = M^{-\frac{1}{2}}$ . While this is a somewhat arbitrary choice, we have found that it works well in practice and defer a more detailed hyperparameter sensitivity analysis to Section S3 of the Supplementary Materials.

### 5.1 Performance in cross-sectional settings

**Covariate effect recovery.** We consider two data generating processes, one with  $p = 3$  correlated covariates and  $R = 2$  effect modifiers (hereafter referred to as the “p3R2” setting) and one with  $p = R = 5$  covariates and modifiers (hereafter referred to as the “p5R5” setting). In both settings, we generated  $n = 2,500$  total observations from the cross-sectional VC model in (2) with  $\sigma = 1$ . We drew the vector of correlated covariates  $\mathbf{x} \sim \mathcal{N}(\mathbf{0}_p, \Sigma_X)$  where the  $(j, k)$  entry of  $\Sigma_X$  is  $0.75^{|j-k|}$ . In the p3R2 setting, we drew the vector of effect modifiers uniformly from the product space  $[0, 1] \times \{0, 1\}$  whereas in the p5R5 setting, we drew the modifiers  $\mathbf{z}$  uniformly from  $[0, 1]^5$ .

The top row of Figure 1 shows the true functions used in the p3R2 setting. For the p5R5

setting, we use the following covariate effect functions:

$$\begin{aligned}\beta_0(\mathbf{z}) &= 3z_1 + (2 - 5 \times \mathbf{1}(z_2 > 0.5)) \sin(\pi z_1) - 2 \times \mathbf{1}(z_2 > 0.5) \\ \beta_1(\mathbf{z}) &\sim \text{GP}(0, K) \\ \beta_2(\mathbf{z}) &= (3 - 3z_1^2 \cos(6\pi z_1)) \times \mathbf{1}(z_1 > 0.6) - 10\sqrt{z_1} \times \mathbf{1}(z_1 < 0.25) \\ \beta_3(\mathbf{z}) &= (1 - z_3)^{\frac{1}{3}} \sin(3\pi(1 - z_4)) - \sqrt{1 - z_1} \\ \beta_4(\mathbf{z}) &= 10 \sin(\pi z_1 z_2) + 20(z_3 - 0.5)^2 + 10z_4 + 5z_5 \\ \beta_5(\mathbf{z}) &= \exp\{\sin((0.9(z_1 + 0.48))^{10})\} + z_2 z_3 + z_4.\end{aligned}$$

We drew the function  $\beta_1$  from a Gaussian process whose covariance kernel was the product of a squared exponential and periodic kernel function. We used the functions  $\beta_0, \beta_1$ , and  $\beta_2$  in both the p3R2 and p5R5 setting. The functions  $\beta_4$  and  $\beta_5$  are due to [Friedman \(1991\)](#) and [Gramacy and Lee \(2009\)](#) respectively.

The second row of [Figure 1](#) superimposes the VC-BART posterior mean and pointwise 95% credible intervals over the true functions. Though the true functions display markedly different behaviors, VC-BART recovers each rather well: the posterior means of each  $\beta_j$  closely track the true functions and, for the most part, the true function values lie within the shaded pointwise 95% credible intervals.

[Table 1](#) compares the VC-BART’s out-of-sample covariate function recovery performance to that of the standard linear model (implemented as `lm` in R), [Li et al. \(2013\)](#)’s kernel smoothing (implemented in the `np` package by [Hayfield and Racine \(2008\)](#)), and [Zhou and Hooker \(2019\)](#)’s boosted tree procedure method (tbVCM; R code available at <https://github.com/siriuz42/treeboostVCM>) averaged over 50 random 75% – 25% training/testing splits of the data. We measured function recovery performance with the mean square error (MSE) averaged over all test observation and across all of the functions  $\beta_j$ . We also measured the frequentist coverage of each method’s 95% uncertainty intervals as well as the lengths of each method’s uncertainty intervals relative to the length of the corresponding VC-BART credible intervals. Relative lengths greater than one indicate that a particular method is more uncertain about its estimates of  $\beta_j(\mathbf{z})$  than VC-BART. Since off-the-shelf implementations of kernel smoothing and tbVCM do not return standard errors of the estimated  $\hat{\beta}_j(\mathbf{z})$ ’s, we estimated these standard errors with the bootstrap. We then used these standard error estimates to form asymptotic 95% confidence intervals. [Table 1](#) reports the MSE, coverage, and relative lengths of the uncertainty intervals averaged over all of the test set observations

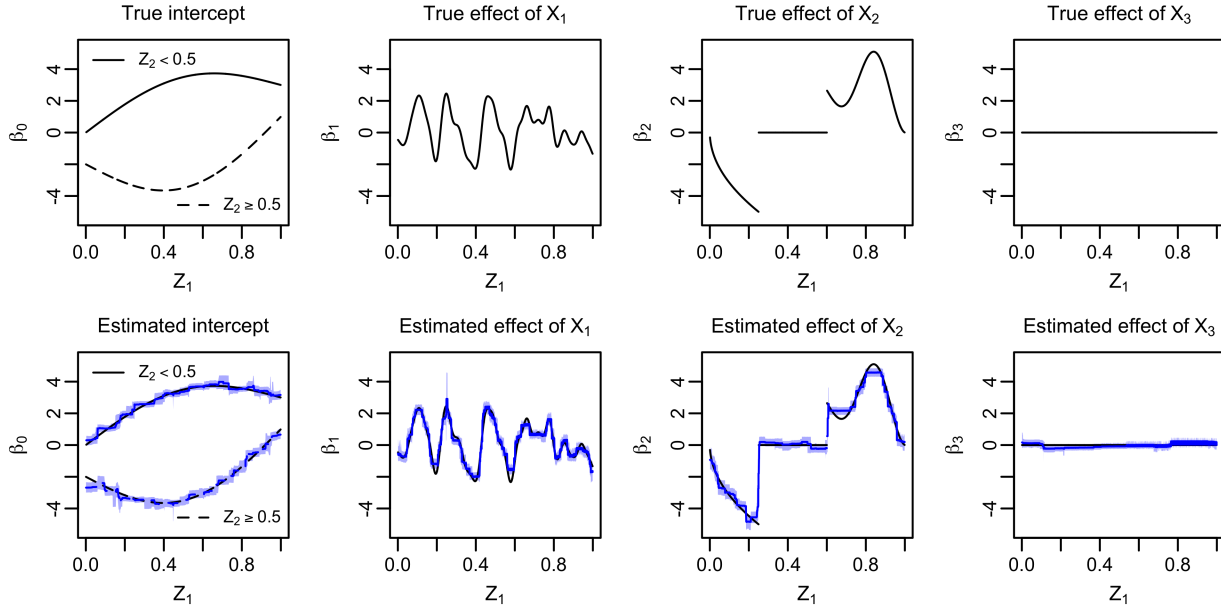


Figure 1: Top row: True intercept and covariate effect functions used in the p3R2 setting. Bottom row: VC-BART’s posterior mean (blue line) and pointwise 95% credible interval (shaded) for each function.

and across all functions  $\beta_j$ . We report the function-by-function performance in Section S4 of the Supplementary Materials.

In both the p3R2 and p5R5 settings, VC-BART produces more accurate points estimates of  $\beta_j(\mathbf{z})$  and is less uncertain about these estimates than kernel smoothing and tbVCM. While the bootstrapped confidence intervals for tbVCM appear to have the best frequentist coverage of the methods considered, we note that these intervals are several times longer than the corresponding VC-BART credible intervals.

Table 1: MSE, uncertainty interval coverage, and relative length of uncertainty intervals for  $\beta_j$  averaged over all testing observations and functions in the p3R2 and p5R5 settings. Reported measures are averaged over 50 training–testing splits, with standard errors shown in parentheses. Best performance according to each metric is bolded.

Method	MSE	Coverage	Relative Length
p3R2: $n = 2500, p = 3, R = 2$			
lm	4.26 (0.09)	0.37 (0.06)	<b>0.88</b> (0.04)
np	0.14 (0.01)	0.91 (0.01)	1.94 (0.14)
tbVCM	0.46 (0.03)	<b>0.98</b> (0.00)	6.18 (0.28)
VC-BART	<b>0.06</b> (0.01)	0.86 (0.05)	1.00 (0.00)
p5R5: $n = 2500, p = 5, R = 5$			
lm	6.76 (0.17)	0.30 (0.04)	<b>0.95</b> (0.04)
np	1.70 (0.08)	0.80 (0.01)	2.87 (0.15)
tbVCM	2.07 (0.08)	<b>0.86</b> (0.01)	3.78 (0.16)
VC-BART	<b>0.22</b> (0.02)	0.85 (0.02)	1.00 (0.00)

**Predictive performance.** VC-BART also demonstrates excellent out-of-sample predictive performance in cross-sectional setting. Table 2 compares the out-of-sample predictive performance of the VC methods considered above to that of BART (implemented in BART R package by McCulloch et al. (2018)), extremely randomized trees (ERT; implemented in the ranger R package by Wright and Ziegler (2017)), and gradient boosting machines (GBM; implemented in the gbm R package by Greenwell et al. (2019)).

We measured out-of-sample predictive performance with the MSE. We also compare the coverage and relative lengths of the pointwise 95% predictive intervals. For the two Bayesian methods, VC-BART and BART, this involved computing quantiles after simulating posterior predictive draws. With the exception of the linear model, the default implementations of all of the non-Bayesian methods we considered do not return any measure of predictive uncertainty. For these methods, we computed the root mean square error (RMSE) on the training data and took  $\hat{y}^* \pm 1.96 \times \text{RMSE}$  as an approximate predictive interval, recognizing that there is no *a priori* reason to expect that such will have nominal coverage. Like in Table 1, we report the average ratio of the lengths of these prediction intervals to VC-BART’s posterior predictive intervals; values larger than one indicate that a method is, on average, more uncertain about its point predictions than VC-BART.



Table 2: Mean square error, predictive interval coverage, and relative length of pointwise predictive intervals for out-of-sample observations  $y^*$ . Reported measures are averaged over 50 training–testing splits, with standard errors shown in parentheses. Run-time is reported in seconds. For **np** and TVCM, the reported time includes the time spent bootstrapping standard errors of  $\hat{\beta}(\mathbf{z}_i)$ . Best performance according to each measure is bolded.

Method	MSE	Coverage	Relative Length	Time
p3R2				
lm	16.88 (0.79)	<b>0.96</b> (0.01)	3.85 (0.04)	<b>0.00</b> (0.00)
np	1.29 (0.1)	0.90 (0.02)	0.86 (0.02)	137.3 (59.36)
tbVCM	1.65 (0.13)	0.74 (0.02)	0.67 (0.01)	2113.84 (189.09)
BART	1.92 (0.18)	<b>0.96</b> (0.01)	1.29 (0.02)	27.11 (16.45)
Extra Trees	3.57 (0.3)	0.82 (0.02)	1.07 (0.01)	0.49 (0.43)
GBM	2.32 (0.18)	0.69 (0.02)	<b>0.65</b> (0.03)	38.1 (20.49)
VC-BART	<b>1.15</b> (0.07)	0.95 (0.01)	1.00 (0.00)	213.57 (83.72)
p5R5				
lm	48.68 (3.22)	0.95 (0.01)	4.84 (0.09)	<b>0.01</b> (0.01)
np	7.91 (0.64)	0.67 (0.03)	0.89 (0.06)	3766.73 (2912.55)
tbVCM	6.14 (0.54)	0.4 (0.02)	<b>0.40</b> (0.02)	3931.21 (853.71)
BART	6.27 (0.46)	0.97 (0.01)	1.79 (0.05)	34.48 (27.52)
Extra Trees	27.76 (2.61)	0.79 (0.02)	1.99 (0.04)	0.77 (0.58)
GBM	8.23 (0.89)	0.47 (0.03)	0.51 (0.02)	48.02 (30.5)
VC-BART	<b>1.86</b> (0.13)	<b>0.97</b> (0.01)	1.00 (0.00)	488.50 (255.97)

We find that VC-BART has superior out-of-sample predictive performance relative to the flexible blackbox methods. It is further encouraging to see that VC-BART’s predictive uncertainty intervals have excellent frequentist coverage and are, on average, somewhat shorter than BART’s.

## 5.2 The panel setting and misspecified error correlation structure

We now investigate how potential misspecification of the error correlation structure affects VC-BART’s performance in the panel setting. For simplicity, for each of  $n = 25$  subjects, we generated 20 training observations and five testing observations at equally-spaced time points from (3) using the same covariate effect functions from the p3R2 setting above. We also drew the  $p = 3$  correlated predictors and  $R = 2$  modifiers in exactly the same fashion described above. We generated errors with an AR(1) correlation structure with  $\rho_{\text{true}} = 0.75$  and ran two chains of our conditional Gibbs sampler with the correctly specified error correlation structure and autocorrelation  $\rho$ .

We systematically assess VC-BART’s sensitivity to misspecified autocorrelation  $\rho$  and/or misspecified error correlation structure as follows. We first run chains of our sampler with the correctly specified AR(1) error, with misspecified autocorrelation  $\rho \in \{0, 0.1, 0.2, \dots, 0.9\}$ . We then run chains with misspecified compound symmetry (CS) error structure, across the same grid of  $\rho$ . In all, we compare the performance of our conditional Gibbs sampler under 21 different settings.

As in the previous subsection, we compare the out-of-sample mean square error and the frequentist coverage and relative lengths of the pointwise 95% uncertainty intervals, averaged across all test observations. In these experiments, we compare the lengths of the uncertainty intervals produced by each setting of our Gibbs sampler to the lengths of the uncertainty intervals produced by the Gibbs sampler run with the correctly specified error distribution. As a result, relative length values substantially larger than one indicate that misspecifying the value of  $\rho$  or the functional form of  $\Sigma_i(\rho)$  results in more posterior uncertainty.

Figure 2 illustrates the sensitivity of VC-BART’s performance to misspecification of the error distribution. We visualize the performance across 10 Monte Carlo replications as a function of the value of  $\rho$  used to run VC-BART. Circles correspond to the average performance when we run VC-BART with an AR(1) error correlation structure while triangles correspond to performance when we run VC-BART with a CS error correlation structure. The shaded regions cover one standard deviation on either side of the mean performance. The average performance of VC-BART run with a correctly specified error distribution is shown with a black asterisk.

In terms of estimating the covariate effects, running VC-BART with a misspecified CS error correlation structure generally yielded slightly worse MSE than running it with a correctly specified AR structure. However, the overall coverage of the credible intervals for the  $\beta_j(\mathbf{z})$ ’s was fairly insensitive to misspecification of either the autocorrelation  $\rho$  or error correlation structure. Interestingly, the substantial overlap in the shaded regions of the predictive MSE (bottom left panel) suggests that out-of-sample point predictions are also rather insensitive to misspecification of the error correlation distribution. We generally observe that as the autocorrelation  $\rho$  increases and  $\Sigma(\rho)$  becomes more and more ill-conditioned, the credible intervals and predictive intervals become wider relative to the correct specification.

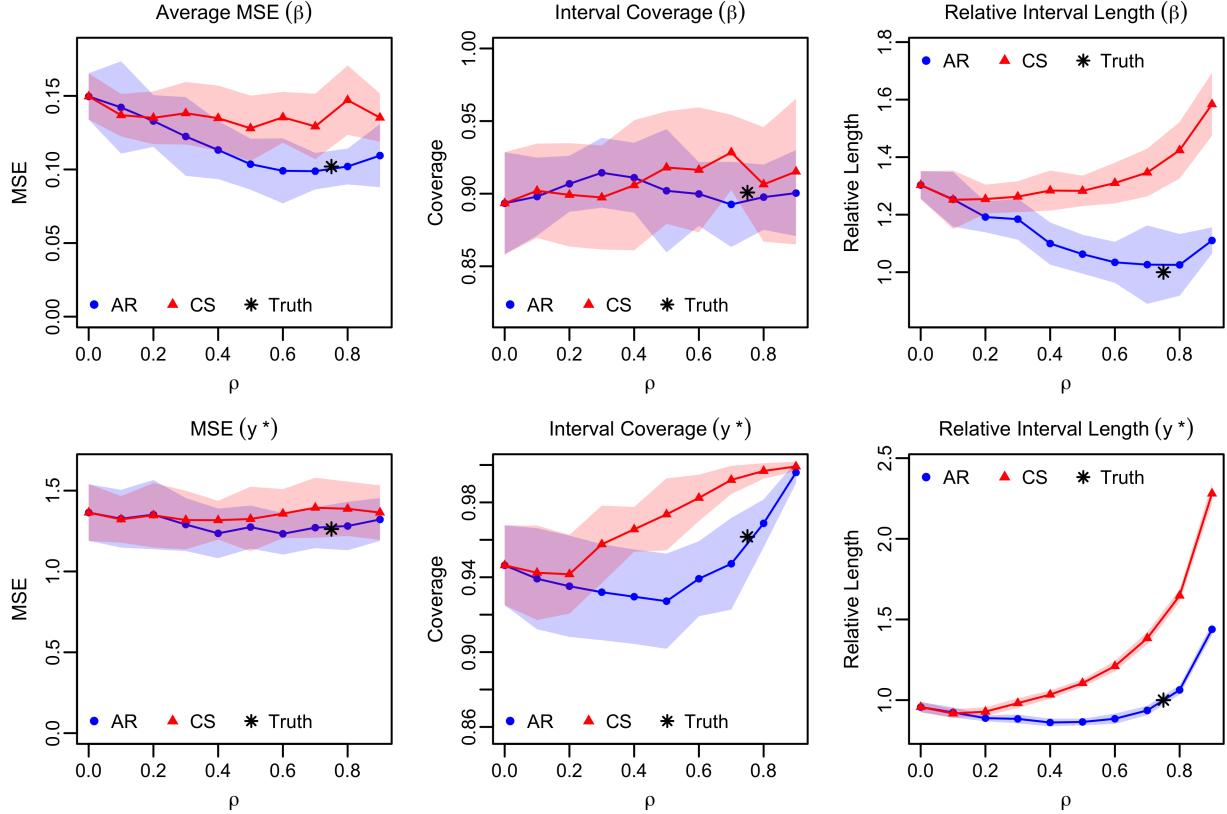


Figure 2: Blue circles show performance of VC-BART run with AR(1) error correlation structure while red triangles show performance of VC-BART run with CS error correlation structure. Values within one standard deviation of the mean performance are shaded. The performance of VC-BART run with a correctly specified error is shown with an asterisk.

## 6 Empirical Illustration

### 6.1 Heterogeneous marginal returns to education

In a seminal 1974 book (Mincer, 1974), Jacob Mincer introduced the Human Capital Earnings Function that predicts a worker’s log wages as a function of his or her years of schooling (*educ*) and years of potential labor market experience (*exper*):

$$\log(wages) = \beta_0 + \beta_1 educ + \beta_2 exper + \beta_3 exper^2 + \sigma \varepsilon.$$

Mincer’s basic log-linear specification has formed the cornerstone of much empirical economic research over the last 40 years. The parameter  $\beta_1$ , referred to as the *return to education*,

captures the effect of an additional year of schooling on earnings. According to [Card \(1999\)](#), it is now commonly accepted that “the return to education is not a single parameter in the population, but rather a random variable that *may vary with other characteristics of individuals, such as family background, ability, or level of schooling*” (emphasis ours).

The cross-sectional VC model allows us to study precisely such structured heterogeneity. Since the quadratic dependence of wages on experience in Mincer’s original equation generally yield poor fits to empirical data ([Murphy and Welch, 1990](#)), we fit a generalized Mincer model to [Wooldridge \(2000\)](#)’s “wage1” dataset:  $\log(wages) = \beta_0(\mathbf{z}) + \beta_1(\mathbf{z})educ + \sigma\varepsilon$ . This dataset, which is available as part of the [Hayfield and Racine \(2008\)](#)’s `np` package, consists of  $n = 526$  randomly selected observations from the 1976 U.S. Current Population Survey. In addition to years of potential labor market experience, our modifier  $\mathbf{z}$  includes the number of years spent with current employer and binary indicators for gender, race, and marital status.

Figure 3(a) shows the out-of-sample mean square error over 50 training/testing splits of the dataset for each of the methods considered in the previous section. It is interesting to see that [Zhou and Hooker \(2019\)](#)’s boosted tree procedure, `tbVCM`, performs quite similarly to fitting Mincer’s original model. We find that in 45 of our 50 replications, VC-BART has a slightly smaller out-of-sample MSE than kernel smoothing. It is perhaps more striking to note that VC-BART displays virtually the same predictive performance as BART, ERT, and GBM. In other words, at least on this dataset, we sacrifice virtually no predictive power when we fit an interpretable VC-BART model rather than a more flexible blackbox model.

Figure 3(b) plots VC-BART’s estimated return on education for two different individuals as a function of potential experience, which is essentially a proxy for age in our dataset. The first individual, whose returns are shown in circles, is a married white female who has worked at her current company for five years. The second individual, whose returns are shown in triangles, is a newly hired unmarried, nonwhite male.

Our results suggest that both individuals’ returns are essentially constant until about middle age, at which point they drop slightly. The fact that none of the 95% credible intervals for either individual contains zero indicates that there is indeed a positive return on education. However, we note that all of the credible intervals are rather wide, indicating substantial uncertainty about the size of the return. In fact, averaged over all levels of potential experience, the intervals span a range of about 7%. Although our estimated return on education for the married white female with five years of tenure is about 1.2 percentage points higher than the return for the newly hired unmarried, nonwhite male, we observe substantial overlap in

the pointwise credible intervals. It is also interesting to see that the return estimated using Mincer’s original specification falls within all of the VC-BART credible interval. In short, our results suggest that while there might be heterogeneity in the return on education, the differences across individuals may be rather small.

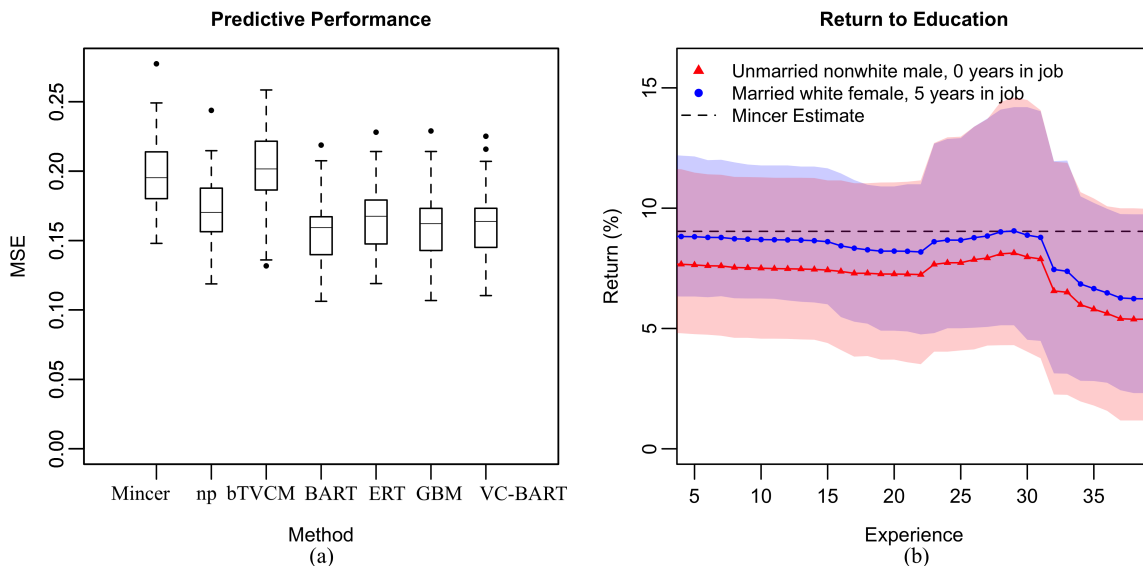


Figure 3: (a) Out-of-sample MSE for each method over 50 training/testing splits of wage1 dataset. (b) Estimated return on education as a function of potential years of experience for a married white female with five years on job (circle) and newly hired unmarried nonwhite male (triangle). 95% credible regions shaded. Dashed lines show the estimated return from Mincer’s original specification.

## 6.2 Spatiotemporal modeling of crime in Philadelphia

While the overall number of violent crimes reported in the city of Philadelphia has fallen over the last decade or so, there is substantial heterogeneity in crime dynamics at the local neighborhood level (Balocchi and Jensen, 2019; Balocchi et al., 2019). Balocchi and Jensen (2019) fit a linear model to predict the crime level within each neighborhood as a function of time and several neighborhood-level predictors. While their model displayed promising predictive capabilities, it assumed (i) that the level of crime in each neighborhood was monotonic in time and in each of the predictors, and (ii) that the effects of time and each predictor were constant over time and space. We now re-analyze a subset of the Philadelphia crime dataset with a panel VC model that relaxes both assumptions.

Our raw crime data comes from the Philadelphia Police Department, which publicly releases the location, time, and type of each reported crime. Following [Balocchi and Jensen \(2019\)](#), we model an essentially logarithmic transformation of violent crime counts aggregated the census tract level over the four year period 2015 – 2018. In all, we have  $n_i = 48$  observations, equally spaced in time, in each of the  $n = 255$  census tracts that comprise the Center City region. We use the same  $p = 6$  covariates as [Balocchi and Jensen \(2019\)](#): the total population, median household income, measures of ethnic segregation and overall poverty, the proportion of vacant land area, and the proportion of commercially-zoned area relative to residentially-zoned area in each census tract. We refer the interested reader to [Balocchi and Jensen \(2019\)](#) for further details on obtaining and pre-processing the crime, economic, land use, and population data used in this analysis.

In our re-analysis, we fit a panel VC model with compound symmetry error correlation structure to the first 42 months of data (January 2015 – June 2018) and assessed the predictive performance on the last six months (July 2018 – December 2018). We considered  $R = 3$  modifiers: the longitude and latitude of the census tract centroids and the time index  $t$ , which ranges from 1 (January 2015) to 48 (December 2018).

Table 3 reports the MSEs for forecasting the crime level in each month of our held out set with VC-BART run with CS error structure and several values of  $\rho$ . In light of our results in Section 5.2, it is interesting to see that running VC-BART with  $\rho = 0$ , essentially assuming that the residual errors are uncorrelated, produced better forecasts of future crime levels. This suggests that the compound symmetry error structure may not be well-specified. Nevertheless, it is encouraging to see that, with  $\rho = 0$ , VC-BART’s predictive performance was on par with BART, ERT, and GBM. In other words, VC-BART produced a more interpretable fit than more flexible blackbox methods without sacrificing any predictive power.

Table 3: MSE of forecasted crime in the six held-out months (July 2018 – December 2018). For VC-BART, the value of the autocorrelation  $\rho$  used is shown in parentheses. During training, the kernel smoothing procedure `np`, causing the default implementation to throw an error. The smallest MSEs in each month and on average are bolded.

Method	07/2018	08/2018	09/2018	10/2018	11/2018	12/2018	Average
lm	1.53	1.50	1.44	1.55	1.51	1.45	1.50
tbVCM	1.17	1.21	1.26	1.40	1.19	1.26	1.25
BART	1.03	1.00	1.01	1.07	1.03	1.06	1.03
ERT	<b>0.99</b>	<b>0.98</b>	1.01	1.07	<b>1.01</b>	1.07	<b>1.02</b>
GBM	<b>0.99</b>	0.99	1.03	1.08	1.02	<b>1.05</b>	1.03
VC-BART (0)	1.01	<b>0.98</b>	<b>1.00</b>	<b>1.05</b>	1.05	1.06	<b>1.02</b>
VC-BART (0.1)	1.06	1.07	1.05	1.11	1.11	1.11	1.09
VC-BART (0.8)	1.35	1.38	1.28	1.38	1.34	1.30	1.34

On the whole, we found that while there was considerable spatial variation in the covariate effects, the temporal variation was often an order of magnitude smaller. For instance, Figure 4 shows the posterior mean effect of log-income on crime levels in each census tract in January 2015, July 2016, and January 2018. In census tracts colored dark blue, a 1% increase in income was associated with an approximately 1.4% decrease in crime; in census tracts colored dark red, a 1% increase in income was associated with a 0.6% increase in crime. We find that for the vast majority of census tracts, the overall change in the effect of income over time was smaller than 0.1 percentage points; in fact, between July 2016 and January 2018, the estimated effect in each census tract changed by less than 0.01 percentage points. That said, we can clearly see several census tracts for which the estimated effect increased rather substantially between January 2015 and July 2016. On closer inspection, however, we found that the monthly 95% credible intervals of these effects contained zero.

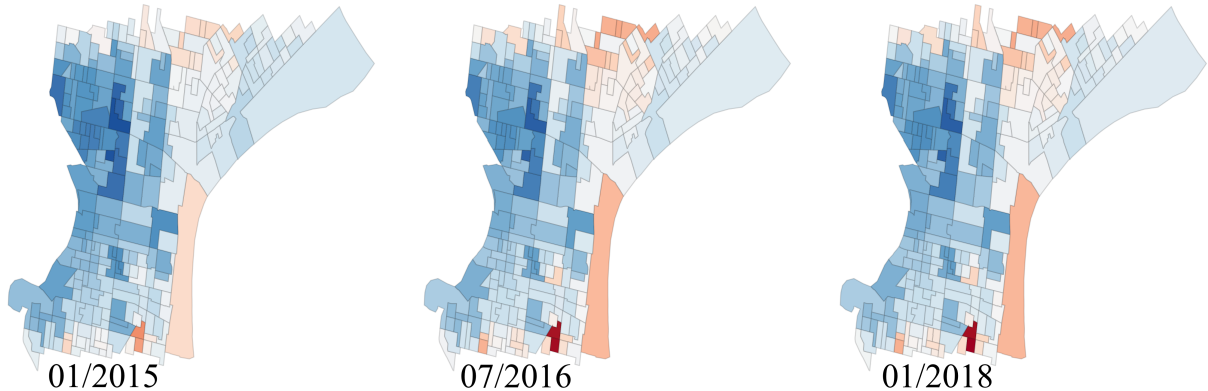


Figure 4: Posterior mean of effect of income in each census tract over time. Light gray lines denote census tract boundaries and each census tract is colored according to the posterior mean.

## 7 Discussion

We have introduced VC-BART for fitting linear varying coefficient models that retain the interpretability of linear models while displaying predictive accuracy on par with more flexible, blackbox regression models. VC-BART achieves covariate effect function recovery and predictive performance superior to existing state-of-the-art VC methods *without intensive problem-specific tuning or imposing any structural assumptions about the functions  $\beta_j(Z)$* . It moreover returns coherent and generally well-calibrated uncertainty quantifications, and enjoys strong theoretical support. Theorems 1 and 2 show that the VC-BART posterior concentrates at close to the minimax optimal rate, losing only a logarithmic factor. This factor stems from not knowing the smoothness of the  $\beta_j$ 's and essentially cannot be improved using our proof techniques. To the best of our knowledge, ours are the first posterior concentration results for the VC model with multivariate modifiers and the first results on the near-optimality of Bayesian treed regression with non-i.i.d. errors. Our results are somewhat stronger than those in Zhou and Hooker (2019), who demonstrate only that their estimates converge in probability to the true functions but do not establish rate-optimality.

There are several exciting avenues for future development and improvement that we briefly mention. Hahn et al. (2020)'s Bayesian causal forest model is a special case of the general VC-BART model with a single, binary covariate that encodes treatment assignment. It would be interesting to study VC-BART's ability to estimate the simultaneous effects of



multiple, possibly continuous, treatments under suitable identifying assumptions.

Since VC-BART approximates the covariate effect functions  $\beta_j$  using piecewise constant functions, it cannot return smooth function estimates. When the true  $\beta_j(\mathbf{z})$ 's are known or suspected to be smoother-than-Lipschitz, one could replace the BART prior in our framework with [Starling et al. \(2019b\)](#)'s tsBART prior, which models the jumps  $\boldsymbol{\mu}$  with a Gaussian process. Alternatively, like [Linero and Yang \(2018\)](#), one could replace the decisions trees in our framework with soft decision trees, in which the internal splits are stochastic. While these modifications are straightforward in principle, they may substantially increase the per-iteration computational complexity.

We have focused primarily on the homoscedastic setting with a common residual standard deviation  $\sigma$  shared across all observations. In the panel data setting, we can easily replace the global  $\sigma$  in Equation (3) with subject-specific standard deviations  $\sigma_i$ , which introduces negligible computational overhead to our Gibbs sampler. Extending [Pratola et al. \(2019\)](#)'s heteroscedastic BART model to allow the  $\sigma$  in Equations (2) and (3) to vary with the covariates and modifiers is a much more ambitious undertaking.

Somewhat more substantively, throughout this work we have assumed that the partition of predictors into sets of covariates  $X$  and effect modifiers  $Z$  was fixed and known. While domain knowledge and theory often suggest natural choices of effect modifiers, we can readily envision scenarios in which it is not immediately clear whether a particular predictor should enter Equation (1) as a covariate, modifier, or both. One potentially promising way to perform modifier selection is to use Dirichlet prior on splitting probabilities like [Linero \(2018\)](#). There are also many applications in which interest lies first in determining whether a covariate has a non-zero effect on the outcome and then estimating how the covariate effect varies with respect to given modifiers. Although VC-BART successfully identified when  $\beta_j(\mathbf{z}) = 0$  in our synthetic experiments, we could replace the fixed  $N(0, \tau_j^2)$  priors on the jumps  $\boldsymbol{\mu}$  with spike-and-slab priors to better facilitate variable selection. Extending VC-BART to perform simultaneous variable and modifier selection along the aforementioned lines is the subject of on-going work.

Estimating the error correlation structure in the panel setting remains an important open problem. Our synthetic experiments suggest that when the VC model is well-specified, point predictions of future observations display little sensitivity to misspecification of the error correlation structure. However, in our analysis of crime in Philadelphia, we found that our predictions noticeably worsened when we increased the autocorrelation  $\rho$  used. In

practice, we recommend running the panel VC-BART model with a fixed error correlation matrix estimate from an initial run of VC-BART with independent errors. That said, a more detailed study of the sensitivity of the panel VC-BART posterior to misspecification of the error correlation structure is certainly warranted. With minor modifications to the MCMC in our VC-BART implementation, it may be possible to use techniques developed by [Giordano et al. \(2018\)](#) to compute local sensitivities without repeatedly refitting the entire model with different error structures.

## References

- Bai, R., Boland, M. R., and Chen, Y. (2019a). Fast algorithms and theory for high-dimensional Bayesian varying coefficient models. arXiv:1907.06477.
- Bai, R., Moran, G. E., Antonelli, J. L., and Boland, M. R. (2019b). Spike-and-slab group lassos for grouped regressions and sparse generalized additive models. arXiv:1907.06477.
- Balocchi, C., Deshpande, S. K., George, E. I., and Jensen, S. T. (2019). Crime in Philadelphia: Bayesian clustering with particle optimization. arXiv:1912.00111.
- Balocchi, C. and Jensen, S. T. (2019). Spatial modeling of trends in crime over time in Philadelphia. *Annals of Applied Statistics*.
- Card, D. (1999). The causal effect of education on earnings. In Ashenfelter, O. and Card, D., editors, *Handbook of Labor Economics*, volume 3. Elsevier Science B.V.
- Chipman, H. A., George, E. I., and McCulloch, R. E. (2010). BART: Bayesian additive regression trees. *The Annals of Applied Statistics*, 4(1):266 – 298.
- Chipman, H. A., George, E. I., McCulloch, R. E., and Shively, T. S. (2019). High-dimensional nonparametric monotone function estimation using BART. arXiv:1612.01619v2.
- Doshi-Velez, F. and Kim, B. (2017). Towards a rigorous science of interpretable machine learning. arXiv:1702.08608v2.
- Eddelbuettel, D. and François, R. (2011). Rcpp: Seamless R and C++ integration. *Journal of Statistical Software*, 40(8):1 – 18.
- Eddelbuettel, D. and Sanderson, C. (2014). Rcpparmadillo: Accelerating R with high-performance C++ linear algebra. *Computational Statistics and Data Analysis*, 71:1054 – 1063.
- Fan, J. and Zhang, W. (2008). Statistical methods with varying coefficient models. *Statistics and its Interface*, 1:179 – 195.
- Franco-Villoria, M., Ventrucci, M., and Rue, H. (2019). A unified view on Bayesian varying coefficient models. arXiv:1806.02084v2.
- Friedman, J. H. (1991). Multivariate adaptive regression splines. *Annals of Statistics*, 19(1):1 – 67.

- Ghosal, S., Ghosh, J. K., and van der Vaart, A. (2000). Convergence rates of posterior distributions. *Annals of Statistics*, 28(2):500 – 531.
- Ghosal, S. and van der Vaart, A. (2017). *Fundamentals of Nonparametric Bayesian Inference*. Cambridge University Press.
- Giordano, R., Broderick, T., and Jordan, M. I. (2018). Covariances, robustness, and variational Bayes. *Journal of Machine Learning Research*, 19(51):1 – 49.
- Gramacy, R. B. and Lee, H. K. H. (2009). Adaptive design and analysis of supercomputer experiments. *Technometrics*, 51(2):130 – 145.
- Greenwell, B., Boehmke, B., Cunningham, J., and GBM Developers (2019). *gbm: Generalized Boosted Regression Models*. R package version 2.1.5.
- Hahn, P. R., Murray, J. S., and Carvalho, C. M. (2020). Bayesian regression models for causal inference: regularization, confounding, and heterogeneous effects. *Bayesian Analysis*.
- Härdle, W., Liang, H., and Guo, J. (2000). *Partially Linear Models*. Physica-Verlag Heidelberg.
- Hastie, T. and Tibshirani, R. (1986). Generalized additive models. *Statistical Science*, 1(3):297 – 318.
- Hastie, T. and Tibshirani, R. (1993). Varying-coefficient models. *Journal of the Royal Statistical Society – Series B (Methodological)*, 55(4):757 – 796.
- Hastie, T. and Tibshirani, R. (2000). Bayesian backfitting. *Statistical Science*, 15(3):196 – 213.
- Hayfield, T. and Racine, J. S. (2008). Nonparameter econometrics: The np package. *Journal of Statistical Software*, 27(5).
- Hill, J. L. (2011). Bayesian Nonparametric Modeling for Causal Inference. *Journal of Computational and Graphical Statistics*, 20(1):217–240.
- Hoover, D. R., Rice, J. A., Wu, C. O., and Yang, L.-P. (1998). Nonparametric smoothing estimates of time-varying coefficient models with longitudinal data. *Biometrika*, 85(4):809 – 822.
- Huang, J. Z., Wu, C. O., and Zhou, L. (2002). Varying-coefficient models and basis function approximations for the analysis of repeated measurements. *Biometrika*, 89(1):111 – 128.

- Lee, K., Lee, Y. K., Park, B. U., and Yang, S. J. (2018). Time-dynamic varying coefficient models for longitudinal data. *Computational Statistics and Data Analysis*, 123:50 – 65.
- Li, Q., Ouyang, D., and Racine, J. S. (2013). Categorical semiparametric varying-coefficient models. *Journal of Applied Econometrics*, 28:551 – 579.
- Li, Q. and Racine, J. S. (2010). Smoothing varying-coefficient estimation and inference for qualitative and quantitative data. *Econometric Theory*, 26(6):1607 – 1637.
- Linero, A. R. (2018). Bayesian regression trees for high-dimensional prediction and variable selection. *Journal of the American Statistical Association*, 113(522):626 – 636.
- Linero, A. R., Sinha, D., and Lipsitz, S. R. (2019). Semiparametric mixed-scale models using shared bayesian forests. arXiv:1809.08521v4.
- Linero, A. R. and Yang, Y. (2018). Bayesian regression tree ensembles that adapt to smoothness and sparsity. *Journal of the Royal Statistical Society – Series B (Methodological)*, 80(5):1087 – 1110.
- Logan, B. R., Sparapani, R., McCulloch, R. E., and Laud, P. W. (2019). Decision making and uncertainty quantification for individualized treatments using Bayesian additive regression trees. *Statistical Methods in Medical Research*, 28(4):1079 – 1093.
- McCulloch, R., Sparapani, R., Gramacy, R., Spanbauer, C., and Pratola, M. (2018). *BART: Bayesian additive regression trees*. R package version 2.1.
- Mincer, J. (1974). *Schooling, experience and earnings*. Columbia University Press.
- Murdoch, W. J., Singh, C., Abbasi-Asl, R., and Yu, B. (2019). Interpretable machine learning: definitions, methods, and applications. arXiv:1901.04592.
- Murphy, K. M. and Welch, F. (1990). Empirical age-earnings profiles. *Journal of Labor Economics*, 8(2):202 – 229.
- Murray, J. S. (2019). Log-linear Bayesian additive regression trees for categorical and count response. arXiv:1701.01503v2.
- Park, B. U., Mammen, E., Lee, Y. K., and Lee, E. R. (2015). Varying coefficient regression models: A review and new developments. *International Statistical Review*, 83(1):36 – 64.
- Pratola, M. T., Chipman, H. A., George, E. I., and McCulloch, R. E. (2019). Heteroscedas-

- tic bart using multiplicative regression trees. *Journal of Computational and Graphical Statistics*.
- R Core Team (2019). *R: A language and environment for statistical computing*. R Foundation for Statistical Computing, Vienna, Austria.
- Ročková, V. and Saha, E. (2019). On theory for bart. In Chaudhuri, K. and Sugiyama, M., editors, *Proceedings of Machine Learning Research*, volume 89 of *Proceedings of Machine Learning Research*, pages 2839–2848. PMLR.
- Ročková, V. and van der Pas, S. (2019). Posterior concentration for Bayesian regression trees and forests. *Annals of Statistics*.
- Sivaganesan, S., Müller, P., and Huang, B. (2017). Subgroup finding via Bayesian additive regression trees. *Statistics in Medicine*, 36(15):2391 – 2403.
- Sparapani, R., Logan, B. R., McCulloch, R. E., and Laud, P. W. (2016). Nonparametric survival analysis using Bayesian additive regression trees. *Statistics in Medicine*, 35(16):2741 – 2753.
- Starling, J. E., Aiken, C. E., Murray, J. S., Nakimuli, A., and Scott, J. G. (2019a). Monotone function estimation in the presence of extreme data coarsening: analysis of preeclampsia and birth weight in urban uganda. arXiv:1912.06946.
- Starling, J. E., Murray, J. S., Carvalho, C. M., Bukowski, R., and Scott, J. G. (2019b). Bart with targeted smoothing: an analysis of patient-specific stillbirth risk. arXiv:1805.07656v7.
- Tan, Y. V. and Roy, J. (2019). Bayesian additive regression trees and the General BART model. arXiv:1901.07504v1.
- Tibshirani, R. and Friedman, J. (2019). A pliable lasso. *Journal of Computational and Graphical Statistics*.
- Wang, H. and Xia, Y. (2009). Shrinkage estimation for the varying coefficient model. *Journal of the American Statistical Association*, 104(486):747 – 757.
- Wang, J. C. and Hastie, T. (2012). Boosted varying-coefficient regression models for product demand prediction. *Journal of Computational and Graphical Statistics*, 23(2):361 – 382.
- Wang, L., Li, H., and Huang, J. Z. (2008). Variable selection in nonparametric varying-

- coefficient models for analysis of repeated measurements. *Journal of the American Statistical Association*, 103(484):1556 – 1569.
- Wei, F., Huang, J., and Li, H. (2011). Variable selection and estimation in high-dimensional varying-coefficient models. *Statistica Sinica*, 21:1515 – 1540.
- Wooldridge, J. M. (2000). *Introductory Econometrics: A Modern Approach*. South-Western College Publishing.
- Wright, M. N. and Ziegler, A. (2017). ranger: A fast implementation of random forests for high dimensional data in C++ and R. *Journal of Statistical Software*, 77(1):1 – 17.
- Wu, C. O. and Chiang, C.-T. (2000). Kernel smoothing on varying coefficient models with longitudinal dependent variable. *Statistica Sinica*, 10:433 – 456.
- Xu, D., Daniels, M. J., and Winterstein, A. G. (2016). Sequential BART for imputation of missing covariates. *Biostatistics*, 17(3):589 – 602.
- Zhou, Y. and Hooker, G. (2019). Tree boosted varying coefficient models. arXiv:1904.01058v1.

# Supplementary Materials

## S1 Gibbs Sampler Details

We derive the cross-sectional VC-BART Gibbs sampler in Section S1.1 and then describe the conditional Gibbs sampler for panel data in Section S1.2.

### S1.1 Cross-sectional Gibbs sampler

Recall that our model is

$$y_i = \beta_0(\mathbf{z}_i) + \sum_{j=1}^p \beta_j(\mathbf{z}_i) x_{ij} + \sigma \varepsilon_i; \quad \varepsilon_i \stackrel{\text{i.i.d.}}{\sim} \mathcal{N}(0, 1) \quad (\text{S1})$$

and that we place an  $\text{BART}(M, \tau_j^2)$  prior on each  $\beta_j$  independently. Let  $\mathcal{E}_j = \{(T_m^{(j)}, \boldsymbol{\mu}_m^{(j)})\}_{m=1}^M$ , be the collection of  $M$  regression trees used to approximate the function  $\beta_j$  and let  $\mathcal{E}$  be the collection  $\{\mathcal{E}_0, \dots, \mathcal{E}_p\}$ .

The joint posterior distribution of  $(\mathcal{E}, \sigma)$  is

$$\pi(\mathcal{E}, \sigma \mid \mathbf{Y}) \propto \sigma^{-n} (\nu + \sigma^2)^{-\frac{\nu+1}{2}} \exp\left\{-\frac{\|\mathbf{R}\|_2^2}{2\sigma^2}\right\} \times \prod_{j=0}^p \prod_{m=1}^M \pi(T_m^{(j)}) \tau_j^{-L_m^{(j)}} \exp\left\{-\frac{\|\boldsymbol{\mu}_m^{(j)}\|_2^2}{2\tau_j^2}\right\}, \quad (\text{S2})$$

where  $L_m^{(j)}$  is the number of leaves in tree  $T_m^{(j)}$  and  $\mathbf{R} = (R_1, \dots, R_n)$  is the vector of *full residuals* with entries

$$R_i = y_i - \sum_{m=1}^M g(\mathbf{z}_i; T_m^{(0)}, \boldsymbol{\mu}_m^{(0)}) - \sum_{j=1}^p \sum_{m=1}^M x_{ij} g(\mathbf{z}_i; T_m^{(j)}, \boldsymbol{\mu}_m^{(j)}).$$

We use a Metropolis–within–Gibbs sampler to simulate posterior draws of  $(\mathcal{E}, \sigma)$ .

**Updating a single tree.** To describe the Gibbs update of a single regression tree, recall the additional notation introduced in Section 3 of the main text: For an arbitrary decision tree  $T$  with  $L$  leaves, let  $X(T)$  be the  $n \times L$  matrix whose  $(i, \ell)$  entry is equal to  $x_{ij}$  if observation  $i$  is associated with leaf  $\ell$  in  $T$  (i.e.  $i \in I(\ell; T)$ ) and is zero otherwise.



Now suppose we are updating the  $m^{\text{th}}$  regression tree  $(T_m^{(j)}, \boldsymbol{\mu}_m^{(j)})$  in the ensemble  $\mathcal{E}_j$  used to approximate  $\beta_j$ . Let  $\mathcal{E}^-$  denote the collection of all remaining  $M(p+1) - 1$  regression trees, where, for notational compactness, we have suppressed the dependence of this collection on the indices  $j$  and  $m$ . Additionally, let  $\mathbf{r} = (r_1, \dots, r_n)^\top$  be the vector of *partial residual*

$$r_i = R_i + x_{ij}g(\mathbf{z}_i; T_m^{(j)}, \boldsymbol{\mu}_m^{(j)}),$$

where we have again suppressed the dependence on  $j$  and  $m$  for brevity. With this notation, we have  $\mathbf{r} = \mathbf{R} + X(T_m^{(j)})\boldsymbol{\mu}_m^{(j)}$ .

For an arbitrary regression tree  $(T, \boldsymbol{\mu})$ , the conditional posterior density given  $\mathbf{Y}$ ,  $\mathcal{E}^-$ , and  $\sigma$  is

$$\begin{aligned} \pi(T, \boldsymbol{\mu} \mid \mathcal{E}^-, \sigma, \mathbf{Y}) &\propto \pi(T)\tau^{-L(T)} \exp \left\{ -\frac{1}{2} [\sigma^{-2}(\mathbf{r} - X(T)\boldsymbol{\mu})^\top (\mathbf{r} - X(T)\boldsymbol{\mu}) + \tau^{-2}\boldsymbol{\mu}^\top \boldsymbol{\mu}] \right\} \\ &\propto \pi(T)\tau^{-L(T)} \exp \left\{ -\frac{1}{2} [\boldsymbol{\mu}^\top \Lambda(T)^{-1}\boldsymbol{\mu} - 2\boldsymbol{\mu}^\top \Theta(T)] \right\} \end{aligned} \quad (\text{S3})$$

where  $\Lambda = [\tau_j^{-2}I_{L(T)} + \sigma^{-2}X(T)^\top X(T)]^{-1}$  and  $\Theta = \sigma^{-2}X(T)^\top \mathbf{r}$ .

Integrating  $\boldsymbol{\mu}$  out of (S3), we compute the marginal posterior mass function of  $T$ :

$$\pi(T \mid \mathbf{Y}, \mathcal{E}^-, \sigma) \propto |\Lambda(T)|^{\frac{1}{2}} \tau^{-L(T)} \exp \left\{ \frac{1}{2} \Theta(T)^\top \Lambda(T) \Theta(T) \right\}.$$

We can also read off the conditional density of  $\boldsymbol{\mu} \mid T$  directly from (S3)

$$\pi(\boldsymbol{\mu} \mid T, \mathbf{Y}, \mathcal{E}^-, \sigma) \propto \exp \left\{ -\frac{1}{2} [\boldsymbol{\mu}^\top \Lambda^{-1}(T)\boldsymbol{\mu} - 2\boldsymbol{\mu}^\top \Theta(T)] \right\},$$

which is proportional to the density of a  $\mathcal{N}(\Lambda(T)\Theta(T), \Lambda(T))$  distribution.

**Updating  $\sigma$ .** We use another Metropolis-Hastings step to draw a new value of  $\sigma$  from its conditional distribution with density

$$\pi(\sigma \mid \mathbf{Y}, \mathcal{E}) \propto (\nu + \sigma^2)^{-\frac{\nu+1}{2}} \sigma^{-n} \exp \left\{ -\frac{\mathbf{R}^\top \mathbf{R}}{2\sigma^2} \right\}.$$

In our MH step, we draw a new proposal from a transition kernel  $Q$  with density

$$q(\sigma) \propto \sigma^{-3-n} \exp \left\{ -\frac{\mathbf{R}^\top \mathbf{R}}{2\sigma^2} \right\}.$$

Note that if  $\sigma \sim Q$ , then  $\sigma^2 \sim \text{Inverse Gamma}(\frac{\nu}{2}, \frac{\mathbf{R}^\top \mathbf{R}}{2})$ . The transition kernel  $Q$  is precisely equal to the conditional posterior distribution of  $\sigma$  that we would have obtained had we placed a non-informative Jeffrey's prior on  $\sigma^2$  with improper density  $\sigma^{-2}$ .

Using the transition kernel  $Q$ , which to the best of our knowledge was first suggested by [Linero and Yang \(2018\)](#), facilitates considerable cancellation in the MH acceptance probability. Indeed, if we draw a new proposal  $\tilde{\sigma} \sim Q$ , then we accept the transition from  $\sigma$  to  $\sigma'$  with probability

$$\alpha(\sigma \rightarrow \sigma') = \left( \frac{\nu + \tilde{\sigma}^2}{\nu + \sigma^2} \right)^{-\frac{1+\nu}{2}} \times \left( \frac{\tilde{\sigma}}{\sigma} \right)^3.$$

**Computational complexity.** The computational complexity of our a single iteration of cross-sectional Gibbs sampler is dominated by the Metropolis-Hastings steps used to update the  $pM$  decision trees in our ensemble. Each of these steps requires computing  $\Lambda(T)$  and  $\Theta(T)$ . Recall, that  $X(T)$  is an extremely sparse matrix – each row contains exactly one non-zero element – and the matrix  $X(T)^\top X(T)$  is diagonal. In fact, the  $\ell^{\text{th}}$  diagonal element of  $X(T)^\top X(T)$  is just the sum of the covariates  $x_{ij}^2$  corresponding to observations associated with leaf  $\ell$ . As a result, we can compute both  $\Lambda(T)$  and  $\Theta(T)$  within a single loop over the  $n$  observations. We can then compute  $\Lambda(T)\Theta(T)$  in  $O(L^2)$  operations. Since the BART prior regularizes the decision trees to be rather shallow, typically  $L \ll \sqrt{n}$ , the computational complexity of drawing a new regression tree is just  $O(n)$ . In other words, the per-iteration complexity of our Gibbs sampler is just  $O(Mnp)$ .

## S1.2 Panel Gibbs Sampler

In the panel data setting, we have  $n_i$  observations of  $n$  subjects and we model for each  $i = 1, \dots, n$ , and  $t = 1, \dots, n_i$

$$y_{it} = \beta_0(\mathbf{z}_{it}) + \sum_{j=1}^p \beta_j(\mathbf{z}_{it})x_{itj} + \sigma\varepsilon_{it}, \tag{S4}$$

where  $\varepsilon_i \sim \mathcal{N}(\mathbf{0}_{n_i}, \Sigma_i(\rho))$  and the diagonal elements of  $\Sigma_i(\rho)$  are equal to one.

The joint posterior density of  $(\boldsymbol{\mathcal{E}}, \sigma, \rho)$  is given by

$$\begin{aligned} \pi(\boldsymbol{\mathcal{E}}, \sigma, \rho \mid \mathbf{Y}) &\propto (\nu + \sigma^2)^{-\frac{\nu+1}{2}} \times \prod_{i=1}^n \sigma^{-n_i} |\Omega_i(\rho)|^{\frac{1}{2}} \exp \left\{ -\frac{\mathbf{R}_i^\top \Omega_i(\rho) \mathbf{R}_i}{2\sigma^2} \right\} \\ &\times \prod_{j=0}^p \prod_{m=1}^M \pi(T_m^{(j)}) \tau_j^{-L_m^{(j)}} \exp \left\{ -\frac{\|\boldsymbol{\mu}_m^{(j)}\|_2^2}{2\tau_j^2} \right\}, \end{aligned} \quad (\text{S5})$$

where  $\Omega_i(\rho) = \Sigma_i^{-1}(\rho)$  and the vector of subject  $i$ 's full residuals  $\mathbf{R}_i = (R_{i1}, \dots, R_{in_i})^\top$  is defined similarly to full residuals  $\mathbf{R}$  in the cross-sectional setting.

It is straightforward to extend the cross-sectional Gibbs described above to sample from the *conditional* posterior distribution of  $(\boldsymbol{\mathcal{E}}, \sigma) \mid \mathbf{Y}, \rho$ . Specifically, we use the same basic strategy to update each individual regression tree, first drawing a new decision tree and then conditionally drawing the new jumps. In the panel setting, conditional posterior density of a single regression tree  $(T, \boldsymbol{\mu})$  can also be written as

$$\pi(T, \boldsymbol{\mu} \mid \mathbf{y}, \boldsymbol{\mathcal{E}}^-, \sigma, \rho) \propto \pi(T) \tau^{-L(T)} \exp \left\{ -\frac{1}{2} [\boldsymbol{\mu}^\top \Lambda(T)^{-1} \boldsymbol{\mu} - 2\boldsymbol{\mu}^\top \Theta(T)] \right\}$$

where

$$\begin{aligned} \Lambda(T) &= \left[ \tau^{-2} \mathbf{I}_{L(T)} + \sum_{i=1}^n X_i(T)^\top \Omega_i(\rho) X_i(T) \right]^{-1} \\ \Theta(T) &= \sum_{i=1}^n X_i(T)^\top \Omega_i(\rho) \mathbf{r}_i, \end{aligned}$$

where  $X_i(T)$  is an  $n_i \times L(T)$  matrix whose  $(t, \ell)$  entry is equal to  $x_{ijt}$  if and only if  $\mathbf{z}_{it}$  is associated with leaf  $\ell$  of tree  $T$  and is equal to zero otherwise.

The key difference between the expressions for  $\Lambda(T)$  and  $\Theta(T)$  in the panel and cross-sectional settings is the additional  $\Omega_i(\rho)$  term, corresponding to the inverse correlation matrix of subject  $i$ 's residual errors  $\varepsilon_{it}$ . For a general  $\Omega_i(\rho)$ , the complexity of computing the quadratic form  $X_i(T)^\top \Omega_i(\rho) X_i(T)$  is  $O(n_i^2)$ . This means that the per-iteration complexity of our conditional Gibbs sampler could scale super-linearly in the total number of observations  $N = \sum_{i=1}^n n_i$ .

However, if we assume a compound symmetry error correlation structure, in which all off-diagonal elements of  $\Sigma_i(\rho)$  are equal to  $\rho$ , we can compute this quadratic form with  $O(n_i)$  operations, resulting in a per-iteration complexity of  $O(NMp)$ . Similarly, if we assume an

autoregressive AR(1) error correlation structure and further assume that each individual is observed at equally spaced times  $t_{i,j}$  with  $t_{i,j+1} = t_{i,j} + 1$ , we can also maintain this same complexity.

## S2 Proofs of Main Results

The proofs of Theorems 1 and 2 are based on the standard prior concentration and testing arguments outlined in Ghosal and van der Vaart (2017). Roughly speaking, in order to prove optimal posterior concentration, the prior on  $\boldsymbol{\beta} = [\beta_0, \dots, \beta_p]$  first needs to be “close” enough to  $\boldsymbol{\beta}_0$  (i.e. the prior needs to assign enough positive probability mass to a neighborhood of  $\boldsymbol{\beta}_0$ ). Second, we need to construct exponentially powerful statistical tests, so that the probabilities of Type I and Type II errors for testing  $H_0 : \boldsymbol{\beta} = \boldsymbol{\beta}_0$  vs.  $H_1 : \{\|\boldsymbol{\beta} - \boldsymbol{\beta}_0\|_n > r_n\}$  are exponentially decreasing.

Throughout this section, we use the following notation. For two densities  $f$  and  $g$ , let  $K(f, g) = \int f \log(f/g)$  and  $V(f, g) = \int f |\log(f/g) - K(f/g)|^2$  denote the Kullback-Leibler (KL) divergence and KL variation respectively. Denote the Rényi divergence of order 1/2 as  $\rho(f, g) = -\log \int f^{1/2} g^{1/2} d\nu$ . Finally, denote the  $\varepsilon$ -covering number for a set  $\Omega$  with semimetric  $d$  as the minimum number of  $d$ -balls of radius  $\varepsilon$  needed to cover  $\Omega$  and denote the  $\varepsilon$ -covering number as  $N(\varepsilon, \Omega, d)$  and the metric entropy as  $\log N(\varepsilon, \Omega, d)$ .

### S2.1 Proof of Theorem 1

Let  $\theta_i = \sum_{j=0}^p \beta_j(\mathbf{z}_i) x_{ij}$ , and let  $\boldsymbol{\theta} = (\theta_1, \dots, \theta_n)^\top$  be an  $n \times 1$  vector. Let  $\theta_{0,i} = \sum_{j=0}^p \beta_{0,j}(\mathbf{z}_i) x_{ij}$ , and let  $\boldsymbol{\theta}_0 = (\theta_{0,1}, \dots, \theta_{0,n})^\top$ . Let  $\mathbb{P}_{\boldsymbol{\beta}_0}^{(n)}$  denote the probability measure underlying the true model,

$$y_i = \beta_{0,0}(\mathbf{z}_i) + \sum_{j=1}^p \beta_{0,j} x_{ij} + \sigma_0 \varepsilon_i, \quad i = 1, \dots, n. \quad (\text{S6})$$

For the  $i$ th observation, the response  $y_i$  is distributed as  $y_i \sim \mathcal{N}(\theta_i, \sigma^2)$ . Let  $f_i$  denote the marginal law for  $y_i$  and  $f = \prod_{i=1}^n f_i$ . Analogously, let  $f_{0,i}$  be the marginal law for  $y_i \sim \mathcal{N}(\theta_{0,i}, \sigma^2)$ , and let  $f_0 = \prod_{i=1}^n f_{0,i}$ .

The proof of Theorem 1 can be sketched as follows. Lemma 3 establishes the optimal

prior concentration in terms of KL divergence and variation. Lemma 4 establishes optimal posterior concentration in terms of average Rényi divergence (of order 1/2). We then show that  $\{\frac{1}{n}\rho(f, f_0) > K_1 r_n^2\} \supset \{\boldsymbol{\beta} : \|\boldsymbol{\beta} - \boldsymbol{\beta}_0\|_n^2 > K_2 r_n^2\}$  for sufficiently large  $n$  and some  $K_1, K_2 > 0$ . Since  $\{\frac{1}{n}\rho(f, f_0) > K_1 r_n^2\}$  is an event with asymptotically vanishing posterior probability, this implies that  $\{\boldsymbol{\beta} : \|\boldsymbol{\beta} - \boldsymbol{\beta}_0\|_n^2 > K_2 r_n^2\}$  is as well.

**Lemma 3.** *Under (S6), suppose we endow  $(\boldsymbol{\beta}, \sigma)$  with the VC-BART prior. For the BART priors on the  $\beta_j$ 's,  $j = 0, \dots, p$ , suppose that the splitting probability of a node is  $q(d) = \gamma^d$  for some  $1/N \leq \gamma < 1/2$ , and for the prior on  $\sigma$ , assume  $\nu > 1$ . Assume that Assumptions (A1)-(A3) hold. Then for  $r_n^2 = \log n \sum_{j=0}^p n^{-2\alpha_j/(2\alpha_j+R)}$  and some  $C_1 > 0$ ,*

$$\Pi(K(f_0, f) \leq nr_n^2, V(f_0, f) \leq nr_n^2) \gtrsim \exp(-C_1 nr_n^2). \quad (\text{S7})$$

*Proof of Lemma 3.* The KL divergence between  $f_0$  and  $f$  is

$$K(f_0, f) = \frac{1}{2} \left[ n \left( \frac{\sigma_0^2}{\sigma^2} \right) - n - n \log \left( \frac{\sigma_0^2}{\sigma^2} \right) + \frac{\|\boldsymbol{\theta} - \boldsymbol{\theta}_0\|_2^2}{\sigma^2} \right], \quad (\text{S8})$$

and the KL variation between  $f_0$  and  $f$  is

$$V(f_0, f) = \frac{1}{2} \left[ n \left( \frac{\sigma_0^2}{\sigma^2} \right)^2 - 2n \left( \frac{\sigma_0^2}{\sigma^2} \right) + n \right] + \frac{\sigma_0^2}{(\sigma^2)^2} \|\boldsymbol{\theta} - \boldsymbol{\theta}_0\|_2^2. \quad (\text{S9})$$

We define the two events  $\mathcal{A}_1$  and  $\mathcal{A}_2$  as follows:

$$\mathcal{A}_1 = \left\{ \sigma : n \left( \frac{\sigma_0^2}{\sigma^2} \right) - n - n \log \left( \frac{\sigma_0^2}{\sigma^2} \right) \leq nr_n^2, n \left( \frac{\sigma_0^2}{\sigma^2} \right)^2 - 2n \left( \frac{\sigma_0^2}{\sigma^2} \right) + n \leq nr_n^2 \right\}, \quad (\text{S10})$$

and

$$\mathcal{A}_2 = \left\{ (\boldsymbol{\beta}, \sigma) : \frac{\|\boldsymbol{\theta} - \boldsymbol{\theta}_0\|_2^2}{\sigma^2} \leq nr_n^2, \frac{\sigma_0^2}{(\sigma^2)^2} \|\boldsymbol{\theta} - \boldsymbol{\theta}_0\|_2^2 \leq nr_n^2/2 \right\}. \quad (\text{S11})$$

From (S8)-(S11), we may write  $\Pi(K(f_0, f) \leq r_n^2, V(f_0, f) \leq r_n^2) = \Pi(\mathcal{A}_2|\mathcal{A}_1)\Pi(\mathcal{A}_1)$ , and we may derive lower bounds for  $\Pi(\mathcal{A}_1)$  and  $\Pi(\mathcal{A}_2|\mathcal{A}_1)$  separately. Arguing as in Bai et al. (2019b),  $\mathcal{A}_1 \supset \mathcal{A}_1^*$ , where  $\mathcal{A}_1^* = \{\sigma : \sigma_0/\sqrt{r_n+1} \leq \sigma \leq \sigma_0\}$ . Noting that the prior on  $\sigma$ ,

$\pi(\sigma)$  is the half- $t$  distribution, we may lower bound  $\Pi(\mathcal{A}_1)$  as

$$\begin{aligned}\Pi(\mathcal{A}_1) &\geq \Pi(\mathcal{A}_1^*) \asymp \int_{\sigma_0/\sqrt{r_n+1}}^{\sigma_0} \left(1 + \frac{1}{\nu} \left(\frac{\sigma}{A}\right)^2\right)^{-\frac{\nu+1}{2}} \\ &\geq \left(1 + \frac{\sigma_0^2}{\nu A^2}\right)^{-\frac{\nu+1}{2}} \\ &\succ \exp(-C_1 n r_n^2/2),\end{aligned}\tag{S12}$$

for some  $C_1 > 0$ .

Next, we focus on lower bounding  $\Pi(\mathcal{A}_2|\mathcal{A}_1)$ . Similarly as in the proof of Theorem 2 of [Bai et al. \(2019b\)](#), the left-hand sides for both the inequalities in the set  $\mathcal{A}_2$ , conditional on  $\mathcal{A}_1$ , can be bounded above by a constant multiple of  $\|\boldsymbol{\theta} - \boldsymbol{\theta}_0\|_2^2$ . Thus, there exists some constant  $b_1 > 0$  so that we may lower bound  $\Pi(\mathcal{A}_2|\mathcal{A}_1)$  as

$$\begin{aligned}\Pi(\mathcal{A}_2|\mathcal{A}_1) &\gtrsim \Pi\left(\boldsymbol{\beta} : \|\boldsymbol{\theta} - \boldsymbol{\theta}_0\|_2^2 \leq \frac{n r_n^2}{2b_1}\right) \\ &= \Pi\left(\boldsymbol{\beta} : \sum_{i=1}^n \left[\sum_{j=0}^p \beta_j(\mathbf{z}_i) x_{ij} - \sum_{j=0}^p \beta_{0,j}(\mathbf{z}_i) x_{ij}\right]^2 \leq \frac{n r_n^2}{2b_1}\right) \\ &\geq \Pi\left(\boldsymbol{\beta} : \sum_{i=1}^n \sum_{j=0}^p [\beta_j(\mathbf{z}_i) - \beta_{0,j}(\mathbf{z}_i)]^2 \leq \frac{n r_n^2}{2b_1 D_1^2 (p+1)}\right) \\ &\geq \prod_{j=0}^p \Pi\left(\beta_j : \sum_{i=1}^n [\beta_j(\mathbf{z}_i) - \beta_{0,j}(\mathbf{z}_i)]^2 \leq \frac{n (r_n^j)^2}{2b_1 D_1^2 (p+1)}\right) \\ &= \prod_{j=0}^p \Pi\left(\beta_j : \|\beta_j - \beta_{0,j}\|_n \leq \frac{r_n^j}{D_1 \sqrt{2b_1(p+1)}}\right),\end{aligned}\tag{S13}$$

where  $r_n^j = n^{-\alpha_j/(2\alpha_j+R)} \log^{1/2} n$ ,  $j = 0, \dots, p$ , and we used Assumption (A2) about the uniform boundedness of the covariates and an application of the Cauchy-Schwartz inequality in the third line of the display. Since we want to show that  $\Pi(\mathcal{A}_2|\mathcal{A}_1) \gtrsim \exp(-C_1 n r_n^2/2)$ , it suffices to show (in light of (S13)) that for each functional  $\beta_j$ ,  $j = 0, \dots, p$ ,

$$\Pi\left(\beta_j : \|\beta_j - \beta_{0,j}\|_n \leq \frac{r_n^j}{D_1 \sqrt{2b_1(p+1)}}\right) \gtrsim e^{-C_1 n (r_n^j)^2/2}.\tag{S14}$$

By Assumption (A1) that  $\|f_0\|_\infty \lesssim \log^{1/2} n$ , it follows from equations (6)-(8) in the proof of Theorem 7.1 in [Ročková and Saha \(2019\)](#) that there exists  $C_1 > 0$  such that for each  $j = 0, \dots, p$ , (S14) is lower-bounded by  $e^{-C_1 n (r_n^j)^2 / 2}$ . Thus, it follows from (S13)-(S14) that  $\Pi(\mathcal{A}_2 | \mathcal{A}_1)$  is lower bounded by  $\exp(-C_1 n r_n^2 / 2)$ . Combining this with (S12) yields the desired lower bound in (S7).  $\square$

Next, we prove posterior contraction of  $f$  to the truth  $f_0$  with respect to average Rényi divergence of order 1/2.

**Lemma 4.** *Under (S6), suppose we endow  $(\boldsymbol{\beta}, \sigma)$  with the VC-BART prior. For the BART priors on the  $\beta_j$ 's,  $j = 0, \dots, p$ , suppose that the splitting probability of a node is  $q(d) = \gamma^d$  for some  $1/n \leq \gamma < 1/2$ , and  $\nu > 1$  in the prior on  $\sigma$ . Then under the same conditions as those in Lemma 3, we have for  $r_n^2 = \log n \sum_{j=0}^p n^{-2\alpha_j / (2\alpha_j + R)}$  and some  $C_2 > 0$ ,*

$$\Pi \left( \frac{1}{n} \rho(f, f_0) \geq C_2 r_n^2 | \mathbf{Y} \right) \rightarrow 0, \quad (\text{S15})$$

in  $\mathbb{P}_{f_0}^{(n)}$ -probability as  $n, p \rightarrow \infty$ .

*Proof of Lemma 4.* Following from first principles (see, e.g. [Ghosal and van der Vaart \(2017\)](#)), this statement will be proven if we can establish that for some  $C_1, C_3 > 0$ ,

$$\Pi(K(f_0, f) \leq n r_n^2, V(f_0, f) \leq n r_n^2) \gtrsim \exp(-C_1 n r_n^2), \quad (\text{S16})$$

as well as the existence of a sieve  $\{\mathcal{F}_n\}_{n=1}^\infty$  such that

$$\Pi(\mathcal{F}_n^c) \leq \exp(-C_3 n r_n^2), \quad (\text{S17})$$

and a test function  $\varphi_n$  such that

$$\begin{aligned} \mathbb{E}_{f_0} \varphi_n &\leq e^{-n r_n^2}, \\ \sup_{f \in \mathcal{F}_n: \rho(f, f_0) > C_2 n r_n^2} \mathbb{E}_f (1 - \varphi_n) &\lesssim e^{-n r_n^2 / 16}. \end{aligned} \quad (\text{S18})$$

We already proved (S16) in Lemma 3. To verify (S17), we consider the sieve,

$$\mathcal{F}_n = \left\{ (\boldsymbol{\beta}, \sigma) : 0 < \sigma < e^{C_4 n r_n^2}, \beta_j \in \mathcal{B}_n^j, j = 0, \dots, p \right\},$$

where for each  $j = 0, \dots, p$ ,  $\mathcal{B}_n^j$  is defined as the sieve in the proof of Theorem 7.1 of [Ročková](#)

and Saha (2019), i.e. the union of all functions belonging to the class of functions  $\mathcal{F}_\varepsilon$  (defined in Ročková and van der Pas (2019)) that are supported on a valid ensemble  $\mathcal{VE}$  (Ročková and van der Pas, 2019), where *each* tree in the  $j$ th ensemble  $\mathcal{E}_j$  has at most  $l_n^j$  leaves, and  $l_n^j$  is chosen as  $l_n^j = \lfloor \tilde{C}n(r_n^j)^2/\log n \rfloor \asymp n^{R/(2\alpha_j+R)}$ , for sufficiently large  $\tilde{C} > 0$ . With this sieve, we have

$$\Pi(\mathcal{F}_n^c) \leq \Pi(\sigma > e^{C_4nr_n^2}) + \sum_{j=0}^p \Pi(\beta_j \notin \mathcal{B}_n^j). \quad (\text{S19})$$

Since we assumed that  $\nu > 1$  in the half- $t$  prior on  $\sigma$ ,  $\mathbb{E}(\sigma)$  is well-defined, and a simple application of the Markov inequality gives  $\Pi(\sigma > e^{C_4nr_n^2}) \leq e^{-C_4nr_n^2} \mathbb{E}(\sigma) \lesssim e^{-C_5nr_n^2}$  for some  $C_5 > 0$ . Let  $L_m^j$  denote the number of terminal leaf nodes in the  $m$ th tree of the  $j$ th tree ensemble  $\mathcal{E}_j$  corresponding to the functional  $\beta_j(\mathbf{z})$ . Let  $l_n^{\min} = \min\{l_n^1, \dots, l_n^p\}$ , recalling  $l_n^j = \lfloor \tilde{C}n(\varepsilon_n^j)^2/\log n \rfloor$ . Noting that all the BART priors have the same number of trees  $M$ , we have that the second term in (S19) can be bounded above as

$$\begin{aligned} \sum_{j=0}^p \Pi(\beta_j \notin \mathcal{B}_n^j) &\leq \sum_{j=0}^p \Pi\left(\bigcup_{m=1}^M \{L_m^j > l_n^j\}\right) \\ &\leq \sum_{j=0}^p \sum_{m=1}^M \Pi(L_m^j > l_n^j) \\ &\lesssim M \sum_{j=0}^p e^{-C_l l_n^j \log l_n^j} \\ &\lesssim Mp \exp(-C_l l_n^{\min} \log l_n^{\min}) \\ &= M \exp(\log p - C_l l_n^{\min} \log l_n^{\min}), \end{aligned} \quad (\text{S20})$$

where we used the proof of Theorem 7.1 of Ročková and Saha (2019) for the third line. By our assumption on the growth rate of  $p$  in Assumption (A3), we have that  $Me^{-C_l l_n^{\min} \log l_n^{\min} + \log p + C_5nr_n^2} \rightarrow 0$  as  $n, p \rightarrow \infty$  for sufficiently large  $C_l > 0$  and any  $C_5 > 0$ . Thus, we have from (S20) that the second term on the right-hand side of (S19) is bounded above by  $e^{-C_3nr_n^2}$  for some  $C_3 > 0$ , i.e. (S17) holds.

Now we show the existence of a test function  $\varphi_n$  so that (S18) also holds. As in Bai et al. (2019a), we first consider the most powerful Neyman-Pearson test  $\phi_n = \mathbb{I}\{f_1/f_0 \geq 1\}$  for any  $f_1$  such that  $\rho(f_0, f_1) \geq nr_n^2$ , where  $f_1 = \prod_{i=1}^n f_{1,i}$  and  $f_{1,i}$  is the marginal law for



$y_i \sim \mathcal{N}(\boldsymbol{\theta}_{1,i}, \sigma_1^2)$ . If the average Rényi divergence between  $f_0$  and  $f_1$  is bigger than  $r_n^2$ , then

$$\begin{aligned}\mathbb{E}_{f_0} \phi_n &\leq e^{-n\varepsilon_n^2}, \\ \mathbb{E}_{f_1}(1 - \phi_n) &\leq e^{-n\varepsilon_n^2}.\end{aligned}\tag{S21}$$

By the Cauchy-Schwartz inequality, we have

$$\mathbb{E}_f(1 - \phi_n) \leq \{\mathbb{E}_{f_1}(1 - \phi_n)\}^{1/2} \{\mathbb{E}_{f_1}(f/f_1)^2\}^{1/2},\tag{S22}$$

and thus, following from the second inequality in (S21), we can control the probability of Type II error properly if  $\mathbb{E}_{f_1}(f/f_1)^2 \leq e^{7nr_n^2/8}$ . Next, we show that  $\mathbb{E}_{f_1}(f/f_1)^2$  is bounded above by  $e^{7nr_n^2/8}$  for every density  $f_1$  satisfying

$$\begin{aligned}\|\boldsymbol{\theta} - \boldsymbol{\theta}_1\|_2^2 &\leq \frac{nr_n^2}{16}, \\ |\sigma^2 - \sigma_1^2| &\leq \frac{r_n^2}{2},\end{aligned}\tag{S23}$$

First, we note that

$$\mathbb{E}_{f_1}(f/f_1)^2 = \left(\frac{\sigma_1^2}{\sigma^2}\right)^{n/2} \left(2 - \frac{\sigma^2}{\sigma_1^2}\right)^{-n/2} \exp\left(\frac{\|\boldsymbol{\theta} - \boldsymbol{\theta}_1\|_2^2}{2\sigma_1^2 - \sigma^2}\right).\tag{S24}$$

Now, by the second inequality in (S23),  $|(\sigma^2/\sigma_1^2) - 1| \lesssim r_n^2/2$ , or  $1 - \frac{r_n^2}{2} \lesssim \frac{\sigma^2}{\sigma_1^2} \lesssim 1 + \frac{r_n^2}{2}$ . Thus,  $2\sigma_1^2 - \sigma^2 = \sigma^2(\frac{2\sigma_1^2}{\sigma^2} - 1) \gtrsim 1/2$ . Therefore, from (S24), we can bound  $\mathbb{E}_{f_1}(f/f_1)^2$  from above for sufficiently large  $n$  by

$$\begin{aligned}&\left(\frac{1 - r_n^4/4}{1 - r_n^2}\right)^{n/2} e^{2\|\boldsymbol{\theta} - \boldsymbol{\theta}_1\|_2^2} \\ &\leq \left(1 + \frac{3r_n^2}{2}\right)^{n/2} e^{2\|\boldsymbol{\theta} - \boldsymbol{\theta}_1\|_2^2} \\ &\leq e^{3nr_n^2/4} e^{nr_n^2/8} = e^{7nr_n^2/8},\end{aligned}$$

where in the second line of the display, we used the inequality  $(1 - x^2)/(1 - 2x) \leq 1 + 3x$  for small  $x > 0$ , and we used  $x + 1 \leq e^x$  and the assumptions about  $f_1$  in (S23) in the last line. Combining this with the second inequality in (S21) and (S22) gives

$$\mathbb{E}_f(1 - \phi_n) \lesssim e^{-nr_n^2/16}.$$

Thus, we see from the first inequality in (S21) and the above inequality that the test  $\varphi_n$  satisfying (S18) is obtained as the maximum of all tests  $\phi_n$  described above, for each piece required to cover the sieve. To complete the proof of (S18), we need to show that the metric entropy  $\log N(r_n, \mathcal{F}_n, \rho)$ , i.e. the logarithm of the maximum number of pieces needed to cover  $\mathcal{F}_n$  can be bounded above asymptotically by  $nr_n^2$  (see Lemma D.3 of Ghosal and van der Vaart (2017)). By Assumption (A2), we have that  $\frac{1}{n}\|\boldsymbol{\theta} - \boldsymbol{\theta}_1\|_2^2 \leq D_1^2(p+1) \sum_{j=0}^p \|\beta_j - \beta_{0j}\|_n^2$ . Thus, for densities  $f_1$  satisfying (S23), the metric entropy may be bounded above by

$$\sum_{j=0}^p \log N \left( \frac{r_n}{4D_1\sqrt{p+1}}, \{\beta_j \in \mathcal{F}_n : \|\beta_j - \beta_{0j}\|_n < r_n\}, \|\cdot\|_n \right) + \log N \left( \frac{r_n^2}{2}, \{0 < \sigma^2 < e^{C_4 nr_n^2}\}, |\cdot| \right). \quad (\text{S25})$$

Clearly, the second term in (S25) is upper bounded by a constant factor of  $nr_n^2$ . By modifying the proof of Theorem 7.1 in Ročková and Saha (2019) appropriately, we have for some  $A_1 > 0$  and small  $\delta > 0$  that the first term in (S25) can be upper bounded by

$$\sum_{j=0}^p \left[ (l_n^j + 1)M \log(nRl_n^j) + A_1 M l_n^j \log \left( 972D_2 \sqrt{M(p+1)l_n^j n^{1+\delta/2}} \right) \right], \quad (\text{S26})$$

where  $M$  is the number of trees in each ensemble  $\mathcal{B}_n^j$ . Recalling that  $M$  is fixed,  $l_n^j \asymp n(r_n^j)^2 / \log n$  where  $r_n^j = n^{-\alpha_j/(2\alpha_j+R)} \log^{1/2} n$ , and Assumption (A3) that  $R = O(\log^{1/2} n)$ , we have that each summand in the first term in (S25) is upper bounded by  $n(r_n^j)^2$ , and so (S26) is asymptotically bounded above by  $n \sum_{j=0}^p (r_n^j)^2 = nr_n^2$ . Therefore, from (S25)-(S26), we have for densities  $f_1$  satisfying (S23),

$$\log N(r_n, \mathcal{F}_n, \rho) \lesssim nr_n^2,$$

and so this completes the proof of (S18). Having established (S16)-(S18), it follows that we have posterior contraction with respect to average Rényi divergence, i.e. (S15) holds.  $\square$

With Lemmas 3 and 4, we now have the ingredients to prove Theorem 1.

*Proof of Theorem 1.* The average Rényi divergence of order 1/2 between  $f$  and  $f_0$  can be explicitly written as

$$\frac{1}{n} \rho(f, f_0) = -\log \left[ \frac{\sigma^{1/2} \sigma_0^{1/2}}{((\sigma^2 + \sigma_0^2)/2)^{1/2}} \right] + \frac{\|\boldsymbol{\theta} - \boldsymbol{\theta}_0\|_2^2}{4n(\sigma^2 + \sigma_0^2)}. \quad (\text{S27})$$

Now, as proven in Lemma 4,  $\Pi(n^{-1}\rho(f, f_0) \lesssim r_n^2 | \mathbf{Y}) \rightarrow 1$  in  $\mathbb{P}_{f_0}^{(n)}$ -probability as  $n, p \rightarrow \infty$ , and hence, from (S27), we have that with probability tending to one,

$$-\log \left[ \frac{\sigma^{1/2}\sigma_0^{1/2}}{((\sigma^2 + \sigma_0^2)/2)^{1/2}} \right] \lesssim r_n^2.$$

Define  $h^2(\sigma, \sigma_0) = 1 - \frac{\sigma^{1/2}\sigma_0^{1/2}}{((\sigma^2 + \sigma_0^2)/2)^{1/2}}$ . Then using the inequality  $\log x \leq x - 1$ , we have

$$h^2(\sigma, \sigma_0) \leq -\log(1 - h^2(\sigma, \sigma_0)) \lesssim r_n^2.$$

Noting that

$$\frac{\sigma^{1/2}\sigma_0^{1/2}}{((\sigma^2 + \sigma_0^2)/2)^{1/2}} = \left[ \frac{1}{2} \left( \frac{\sigma}{\sigma_0} + \frac{\sigma_0}{\sigma} \right) \right]^{-1/2},$$

this implies that for sufficiently small  $r_n$  such that  $r_n \rightarrow 0$ ,

$$\frac{1}{2} \left( \frac{\sigma}{\sigma_0} + \frac{\sigma_0}{\sigma} \right) < \left( 1 - \frac{r_n^2}{2} \right)^{-2}.$$

Now, the left-hand side of the above display obtains the global minimum when  $\sigma = \sigma_0$ , which implies that  $|\sigma^2 - \sigma_0^2|$  can be made arbitrarily small as  $r_n \rightarrow 0$ . Now, from (S27), we also have

$$\frac{\|\boldsymbol{\theta} - \boldsymbol{\theta}_0\|_2^2}{n(\sigma^2 + \sigma_0^2)} \lesssim r_n^2.$$

Since  $\sigma^2 + \sigma_0^2 \leq |\sigma^2 - \sigma_0^2| + 2\sigma_0^2 \lesssim r_n^2 + 1$ , this implies that

$$\begin{aligned} r_n^2 &\gtrsim \frac{1}{n} \|\boldsymbol{\theta} - \boldsymbol{\theta}_0\|_2^2 / (1 + r_n^2) \\ &= \frac{1}{n(1 + r_n^2)} \sum_{i=1}^n \left[ \sum_{j=0}^p [\beta_j(\mathbf{z}_i)x_{ij} - \beta_{0,j}(\mathbf{z}_i)x_{ij}] \right]^2 \\ &\gtrsim \frac{1}{n(1 + r_n^2)} \sum_{i=1}^n \sum_{j=0}^p (\beta_j(\mathbf{z}_i) - \beta_{0,j}(\mathbf{z}_i))^2 \\ &\asymp \|\boldsymbol{\beta} - \boldsymbol{\beta}_0\|_n^2, \end{aligned} \tag{S28}$$

where we used Assumption (A2) in the third line and the fact that  $r_n^2 \rightarrow 0$  in the last line

of the display. Thus, from (S28), the posterior is asymptotically supported on the event  $\{\boldsymbol{\beta} : \|\boldsymbol{\beta} - \boldsymbol{\beta}_0\|_n^2 \leq M_1^2 r_n^2\}$  for sufficiently large  $n$  and some large constant  $M_1 > 0$ . This proves the theorem.  $\square$

## S2.2 Proof of Theorem 2

Let  $\theta_{it} = \sum_{j=0}^p \beta_0(\mathbf{z}_{it}) x_{itj}$ , and let  $\boldsymbol{\theta}_i = (\theta_{i1}, \dots, \theta_{in_i})^\top$  denote the  $n_i \times 1$  vector corresponding to the  $i$ th subject. Let  $\boldsymbol{\theta} = (\boldsymbol{\theta}_1^\top, \dots, \boldsymbol{\theta}_n^\top)^\top$  be the  $N \times 1$  vector of all the  $\boldsymbol{\theta}_i$ 's. Let  $\theta_{0,itj} = \sum_{j=0}^p \beta_{0,j}(\mathbf{z}_{it}) x_{itj}$  and define  $\boldsymbol{\theta}_{0,i} = (\theta_{0,i1}, \dots, \theta_{0,in_i})^\top$  and  $\boldsymbol{\theta}_0 = (\boldsymbol{\theta}_{0,1}^\top, \dots, \boldsymbol{\theta}_{0,n}^\top)^\top$ . Let  $\mathbb{P}_{\boldsymbol{\beta}_0}^{(N)}$  denote the probability measure underlying the true model,

$$y_{it} = \beta_{0,0}(\mathbf{z}_{it}) + \sum_{j=0}^p \beta_{0,j}(\mathbf{z}_{it}) x_{itj} + \sigma_0 \varepsilon_{it}, \quad 1 \leq i \leq n, 1 \leq t \leq n_i, \quad (\text{S29})$$

where  $\boldsymbol{\varepsilon}_i = (\varepsilon_{i1}, \dots, \varepsilon_{in_i})' \stackrel{\text{ind}}{\sim} \mathcal{N}_{n_i}(\mathbf{0}_{n_i}, \boldsymbol{\Sigma}_i(\rho_0))$ ,  $\rho_0 \in [0, 1)$ . Recall that  $N = \sum_{i=1}^n n_i$  is the total number of observations.

For the  $i$ th observation, the response  $\mathbf{y}_i = (y_{i1}, \dots, y_{in_i})^\top$  is distributed as  $\mathbf{y}_i \sim \mathcal{N}_{n_i}(\boldsymbol{\theta}_i, \sigma^2 \boldsymbol{\Sigma}_i(\rho_0))$ . Let  $f_i$  denote the marginal law for  $\mathbf{y}_i$  and  $f = \prod_{i=1}^n f_i$ . Analogously, let  $f_{0,i}$  be the marginal law for  $\mathbf{y}_i \sim \mathcal{N}_{n_i}(\boldsymbol{\theta}_{0,i}, \sigma^2 \boldsymbol{\Sigma}_i(\rho_0))$ , and let  $f_0 = \prod_{i=1}^n f_{0,i}$ .

The proof of Theorem 2 uses the same techniques as those used to prove Theorem 1. However, some additional care must be taken to account for the fact that we have within-subject correlations. Below, we establish the optimal *prior* concentration for the VC-BART prior in Lemma 5 and the optimal posterior contraction with respect to average Rényi divergence of order 1/2 in Lemma 6. This will then imply the optimal posterior contraction in the empirical  $\ell_2$  norm.

**Lemma 5.** *Under (S29), suppose we endow  $(\boldsymbol{\beta}, \sigma)$  with the VC-BART prior and the autoregressive parameter  $\rho$  with the uniform prior,  $\rho \sim \mathcal{U}(0, 1)$ . For the BART priors on the  $\beta_j$ 's,  $j = 0, \dots, p$ , suppose that the splitting probability of a node is  $q(d) = \gamma^d$  for some  $1/N \leq \gamma < 1/2$ , and for the prior on  $\sigma$ , assume  $\nu > 1$ . Assume that Assumptions (B1)-(B4) hold. Then for  $r_N^2 = \log N \sum_{j=0}^p N^{-2\alpha_j/(2\alpha_j+R)}$  and some  $\tilde{C}_1 > 0$ ,*

$$\Pi(K(f_0, f) \leq nr_N^2, V(f_0, f) \leq Nr_N^2) \gtrsim \exp(-\tilde{C}_1 Nr_N^2). \quad (\text{S30})$$

*Proof of Lemma 5.* Our proof follows along the same lines as the proof of Lemma 1 in Bai

et al. (2019a), with suitable modifications for the fact that we use BART priors on the functionals  $\beta$ . Denote  $\Sigma_i^* = (\sigma^2/\sigma_0^2)\Sigma_{0i}^{-1/2}\Sigma_i\Sigma_{0i}^{-1/2}$ ,  $i = 1, \dots, n$ . Denote the ordered eigenvalues of  $\Sigma_i^*$  by  $\lambda_{it}$ ,  $1 \leq t \leq n_i$ , and let  $\Sigma^* = \text{diag}(\Sigma_1^*, \dots, \Sigma_n^*)$ . Noting that the  $n$  subjects are independent, we have

$$K(f_0, f) = \frac{1}{2} \left\{ \sum_{i=1}^n \sum_{t=1}^{n_i} (\lambda_{it} - 1 - \log \lambda_{it}) + \frac{\|\Sigma^{-1/2}(\theta - \theta_0)\|_2^2}{\sigma^2} \right\},$$

$$V(f_0, f) = \left[ \sum_{i=1}^n \sum_{t=1}^{n_i} \frac{(1 - \lambda_{it})^2}{2} \right] + \frac{\sigma_0^2}{(\sigma^2)^2} \|\Sigma_0^{1/2}\Sigma^{-1}(\theta - \theta_0)\|_2^2.$$

Define the sets,

$$\tilde{\mathcal{A}}_1 = \left\{ \sigma : \sum_{i=1}^n \sum_{t=1}^{n_i} (\lambda_{ij} - 1 - \log \lambda_{ij}) \leq Nr_N^2, \sum_{i=1}^n \sum_{t=1}^{n_i} (1 - \lambda_{ij})^2 \right\},$$

$$\tilde{\mathcal{A}}_2 = \left\{ (\beta, \sigma) : \frac{\|\Sigma^{-1/2}(\theta - \theta_0)\|_2^2}{\sigma^2} \leq Nr_N^2, \frac{\sigma_0^2}{(\sigma^2)^2} \|\Sigma_0^{1/2}\Sigma^{-1}(\theta - \theta_0)\|_2^2 \leq \frac{Nr_N^2}{2} \right\}.$$

Then  $\Pi(K(f_0, f) \leq Nr_N^2, V(f_0, f) \leq Nr_N^2) = \Pi(\tilde{\mathcal{A}}_2|\tilde{\mathcal{A}}_1)\Pi(\tilde{\mathcal{A}}_1)$ , and so we can consider  $\Pi(\mathcal{A}_2|\mathcal{A}_1)$  separately. Using almost identical arguments as those in the proof of Lemma 1 of Bai et al. (2019a),

$$\Pi(\tilde{\mathcal{A}}_1) \gtrsim \exp(-\tilde{C}_1 Nr_N^2/2), \quad (\text{S31})$$

for some  $\tilde{C}_1 > 0$ . Next we focus on bounding  $\Pi(\tilde{\mathcal{A}}_2|\tilde{\mathcal{A}}_1)$  from below. Similarly as in the proof of Lemma 1 of Bai et al. (2019), the left-hand side for both inequalities in the set  $\tilde{\mathcal{A}}_2$ , conditional on  $\tilde{\mathcal{A}}_1$ , can be bounded above by a constant multiple of  $\|\theta - \theta_0\|_2^2$ . Using the same line of reasoning to show (S13) in Lemma 3 and for some constant  $\tilde{b}_1 > 0$ , we then have as a lower bound for  $\Pi(\tilde{\mathcal{A}}_2|\tilde{\mathcal{A}}_1)$ ,

$$\begin{aligned} \Pi(\tilde{\mathcal{A}}_2|\tilde{\mathcal{A}}_1) &\geq \Pi\left(\beta : \|\theta - \theta_0\|_2^2 \leq \frac{Nr_N^2}{2\tilde{b}_1}\right) \\ &\geq \prod_{j=0}^p \Pi\left(\beta_j : \|\beta_j - \beta_{0,j}\|_N \leq \frac{r_N^j}{D_2\sqrt{2\tilde{b}_1(p+1)}}\right), \end{aligned} \quad (\text{S32})$$

where  $r_N^j = N^{-\alpha_j/(2\alpha_j+R)} \log^{1/2} N$ ,  $j = 0, \dots, p$ . Like Lemma 3, it then suffices to show (in

light of (S32)) that for each function  $\beta_j, j = 0, \dots, p$ ,

$$\Pi \left( \beta_j : \|\beta_j - \beta_{0,j}\|_N \leq \frac{r_N^j}{D_2 \sqrt{2\tilde{b}_1(p+1)}} \right) \gtrsim e^{-\tilde{C}_1 N (r_N^j)^2 / 2}, \quad (\text{S33})$$

which holds due to Assumption (B1) that  $\|f_0\|_\infty \lesssim \log^{1/2} N$  and the proof of Theorem 7.1 of Ročková and Saha (2019). Thus, from (S32)-(S33), we have that  $\Pi(\tilde{\mathcal{A}}_2 | \tilde{\mathcal{A}}_1)$  is lower bounded by  $\exp(-\tilde{C}_1 N r_N^2)$ . Combined with (S31), this yields the desired lower bound in (S30).  $\square$

Next, we prove posterior contraction of  $f$  to the truth  $f_0$  with respect to average Rényi divergence of order  $1/2$ .

**Lemma 6.** *Under (S29), suppose we endow  $(\beta, \sigma)$  with the VC-BART prior and the autoregressive parameter  $\rho$  with the uniform prior,  $\rho \sim \mathcal{U}(0, 1)$ . For the BART priors on the  $\beta_j$ 's,  $j = 0, \dots, p$ , suppose that the splitting probability of a node is  $q(d) = \gamma^d$  for some  $1/N \leq \gamma < 1/2$ , and for the prior on  $\sigma$ , assume  $\nu > 1$ . Assume that Assumptions (B1)-(B4) hold. Then for  $r_N^2 = \log N \sum_{j=0}^p N^{-2\alpha_j / (2\alpha_j + R)}$  and some  $\tilde{C}_2 > 0$ ,*

$$\Pi \left( \frac{1}{N} \rho(f, f_0) \geq \tilde{C}_2 r_N^2 | \mathbf{Y} \right) \rightarrow 0, \quad (\text{S34})$$

in  $\mathbb{P}_{f_0}^{(N)}$  probability as  $N, p \rightarrow \infty$ .

*Proof of Lemma 6.* Similar to the proof of Lemma 4, this statement will be proven if we can establish that for some  $\tilde{C}_1, \tilde{C}_3 > 0$ ,

$$\Pi (K(f_0, f) \leq N r_N^2, V(f_0, f) \leq N r_N^2) \gtrsim \exp(-\tilde{C}_1 N r_N^2), \quad (\text{S35})$$

as well as the existence of a sieve  $\{\tilde{\mathcal{F}}_N\}_{N=1}^\infty$  such that

$$\Pi(\tilde{\mathcal{F}}_N^c) \leq \exp(-\tilde{C}_3 N r_N^2), \quad (\text{S36})$$

and a test function  $\tilde{\varphi}_n$  such that

$$\begin{aligned} \mathbb{E}_{f_0} \tilde{\varphi}_N &\leq e^{-N r_N^2}, \\ \sup_{f \in \mathcal{F}_N : \rho(f, f_0) > C_2 N r_N^2} \mathbb{E}_f (1 - \tilde{\varphi}_N) &\lesssim e^{-N r_N^2 / 16}. \end{aligned} \quad (\text{S37})$$

We already proved (S35) in Lemma 5. To verify (S36), we consider the sieve,

$$\tilde{\mathcal{F}}_n = \left\{ (\boldsymbol{\beta}, \sigma, \rho) : 0 < \sigma < e^{\tilde{C}_4 N r_N^2}, e^{-\tilde{C}_4 N r_N^2} < \rho < 1 - e^{-\tilde{C}_4 N r_N^2}, \beta_j \in \tilde{\mathcal{B}}_N^j, j = 0, \dots, p \right\},$$

where for each  $j = 0, \dots, p$ ,  $\tilde{\mathcal{B}}_N^j$  is defined as the sieve in the proof of Theorem 7.1 of Ročková and Saha (2019), i.e. the union of all functions belonging to the class of functions  $\mathcal{F}_\varepsilon$  (defined in Ročková and van der Pas (2019)) that are supported on a valid ensemble  $\mathcal{VE}$  (Ročková and van der Pas, 2019), where *each* tree in the  $j$ th ensemble  $\mathcal{E}_j$  has at most  $l_N^j$  leaves, and  $l_N^j$  is chosen as  $l_N^j = \lfloor \tilde{D} n (r_N^j)^2 / \log N \rfloor \asymp N^{R/(2\alpha_j + R)}$ , for sufficiently large  $\tilde{D} > 0$ . Using very similar steps as those in the proof of Lemma 4, it is clear that  $\Pi(\tilde{\mathcal{F}}_N^c) \leq \exp(-\tilde{C}_3 N r_N^2)$ , i.e. (S36) holds.

Now we show the existence of a test function  $\varphi_n$  so that (S37) also holds. As in Bai et al. (2019a), we first consider the most powerful Neyman-Pearson test  $\phi_n = \mathbb{I}\{f_1/f_0 \geq 1\}$  for any  $f_1$  such that  $\rho(f_0, f_1) \geq N r_N^2$ , where  $f_1 = \prod_{i=1}^n f_{1,i}$  and  $f_{1,i}$  is the marginal law for  $\mathbf{y}_i \sim \mathcal{N}_{n_i}(\boldsymbol{\theta}_{1,i}, \sigma_1^2 \boldsymbol{\Sigma}_i(\rho_1))$ . If the average Rényi divergence between  $f_0$  and  $f_1$  is bigger than  $r_N^2$ , then

$$\begin{aligned} \mathbb{E}_{f_0} \phi_n &\leq e^{-N \varepsilon_N^2}, \\ \mathbb{E}_{f_1} (1 - \phi_n) &\leq e^{-N \varepsilon_N^2}. \end{aligned} \tag{S38}$$

By the Cauchy-Schwartz inequality, we have

$$\mathbb{E}_f (1 - \phi_N) \leq \{\mathbb{E}_{f_1} (1 - \phi_N)\}^{1/2} \{\mathbb{E}_{f_1} (f/f_1)^2\}^{1/2}, \tag{S39}$$

and thus, following from the second inequality in (S38) and (S39), we can control the probability of Type II error properly if  $\mathbb{E}_{f_1} (f/f_1)^2 \leq e^{7N r_N^2/8}$ . Using Assumptions (B2) and (B4) and the same arguments as those in the proof of Lemma 2 in Bai et al. (2019a), we have that  $\mathbb{E}_{f_1} (f/f_1)^2$  is bounded above by  $e^{7N r_N^2/8}$  for densities  $f_1$  satisfying

$$\begin{aligned} \|\boldsymbol{\theta} - \boldsymbol{\theta}_1\|_2^2 &\leq \frac{N r_N^2}{16}, \\ \frac{1}{n} \|\sigma^2 \boldsymbol{\Sigma}(\rho) - \sigma_1^2 \boldsymbol{\Sigma}(\rho_1)\|_F^2 &\leq \frac{r_N^4}{4n_{\max}^2}. \end{aligned} \tag{S40}$$

Combining this with the second inequality in (S38) and (S39) gives

$$\mathbb{E}_f (1 - \phi_N) \lesssim e^{-N r_N^2/16}.$$

Thus, we see from the first inequality in (S38) and the above inequality that the test  $\varphi_N$

satisfying (S37) is obtained as the maximum of all tests  $\phi_N$  described above, for each piece required to cover the sieve. To complete the proof of (S37), we need to show that the metric entropy,  $\log N(r_N, \tilde{\mathcal{F}}_N, \rho(\cdot))$ , i.e. the logarithm of the maximum number of pieces needed to cover  $\tilde{\mathcal{F}}_N$  can be bounded above asymptotically by  $Nr_N^2$ . By Assumption (B2), we have that  $\frac{1}{N}\|\boldsymbol{\theta} - \boldsymbol{\theta}_1\|_2^2 \leq D_2^2(p+1)\sum_{j=0}^p\|\beta_j - \beta_{0j}\|_N^2$ , and by Assumption (B4), the left-hand side of the second inequality in (S40) is bounded above by  $n_{\max}^2(\sigma^2 - \sigma_1^2)^2 + e^{2\tilde{C}_4Nr_N^2}n_{\max}^4(\rho - \rho_1)^2$  on  $\tilde{\mathcal{F}}_N$ . Thus, for densities  $f_1$  satisfying (S40), the metric entropy can be bounded above by

$$\begin{aligned} & \sum_{j=0}^p \log N \left( \frac{r_N}{4D_2\sqrt{p+1}}, \{\beta_j \in \tilde{\mathcal{F}}_N : \|\beta_j - \beta_{0j}\|_N < r_N\}, \|\cdot\|_N \right) \\ & + \log N \left( \frac{r_N^2}{\sqrt{8}n_{\max}^2}, \{\sigma^2 : 0 < \sigma^2 < e^{\tilde{C}_4Nr_N^2}\}, |\cdot| \right) \\ & + \log N \left( \frac{r_N^2}{\sqrt{8}n_{\max}^3 e^{\tilde{C}_4Nr_N^2}}, \{\rho : 0 < \rho < 1\}, |\cdot| \right). \end{aligned} \quad (\text{S41})$$

One can easily verify that the last two terms in (S41) are upper bounded by a constant factor of  $Nr_N^2$ . By modifying the proof of Theorem 7.1 in Ročková and Saha (2019) appropriately, we have for some  $A_2 > 0$  and small  $\delta > 0$  that the first term in (S41) can be upper bounded by

$$\sum_{j=0}^p \left[ (l_N^j + 1)M \log(NRl_N^j) + A_2 M l_N^j \log \left( 972D_2 \sqrt{M(p+1)l_N^j N^{1+\delta/2}} \right) \right], \quad (\text{S42})$$

where  $M$  is the number of trees in each ensemble  $\mathcal{B}_N^j$ . Recalling that  $M$  is fixed,  $l_N^j \asymp N(r_N^j)^2 / \log N$  where  $r_N^j = N^{-\alpha_j/(2\alpha_j+R)} \log^{1/2} N$ , and Assumption (B3) that  $R = O(\log^{1/2} N)$ , we have that each summand in the first term in (S41) is upper bounded by  $N(r_N^j)^2$ , and so (S42) is asymptotically bounded above by  $N\sum_{j=0}^p(r_N^j)^2 = Nr_N^2$ . Therefore, from (S41)-(S42), we have for densities  $f_1$  satisfying (S40),

$$\log N(r_N, \tilde{\mathcal{F}}_N, \rho(\cdot)) \lesssim Nr_N^2,$$

and so this completes the proof of (S37). Having established (S35)-(S37), it follows that we have posterior contraction with respect to average Rényi divergence, i.e. (S34) holds.  $\square$

With Lemmas 5 and 6, we now have the ingredients to prove Theorem 2.



*Proof of Theorem 2.* By Lemma 6,  $\Pi(N^{-1}\rho(f, f_0) \lesssim r_N^2 | \mathbf{Y}) \rightarrow 1$  in  $\mathbb{P}_{f_0}^{(N)}$ -probability as  $N, p \rightarrow \infty$ , where  $\rho(f_0, f)$  is the Rényi divergence of order 1/2. Under our assumptions and following similar arguments as those in the proof of Lemma 3 in Bai et al. (2019a), posterior contraction w.r.t. average Rényi divergence then implies

$$\begin{aligned}
r_N^2 &\gtrsim \frac{1}{N} \|\boldsymbol{\theta} - \boldsymbol{\theta}_0\|_2^2 / (1 + r_N^2) \\
&= \frac{1}{N(1 + r_N^2)} \sum_{i=1}^n \sum_{t=1}^{n_i} \left[ \sum_{j=0}^p [\beta_j(\mathbf{z}_{ij})x_{itj} - \beta_{0,j}(\mathbf{z}_{ij})x_{itj}] \right]^2 \\
&\gtrsim \frac{1}{N(1 + r_N^2)} \sum_{i=1}^n \sum_{t=1}^{n_i} \sum_{j=0}^p (\beta_j(\mathbf{z}_{ij}) - \beta_{0,j}(\mathbf{z}_{ij}))^2 \\
&\asymp \|\boldsymbol{\beta} - \boldsymbol{\beta}_0\|_N^2, \tag{S43}
\end{aligned}$$

where we used Assumption (B2) in the third line and the fact that  $r_N^2 \rightarrow 0$  in the last line of the display. Thus, from (S43), the posterior is asymptotically supported on the event  $\{\boldsymbol{\beta} : \|\boldsymbol{\beta} - \boldsymbol{\beta}_0\|_N^2 \leq M_2^2 r_N^2\}$  for sufficiently large  $N$  and some large constant  $M_2 > 0$ . This proves the theorem.  $\square$

### S3 Hyperparameter Sensitivity

Recall from the main text, that we place a  $\text{BART}(M, \tau_j^2)$  prior on the function  $\beta_j$ . We recommend setting  $M = 50$  and  $\tau_j = M^{-\frac{1}{2}}$ . Under this specification, the marginal prior on  $\beta_j(\mathbf{z})$  is a standard normal. Of course, if one has strong prior beliefs about the range of standardize covariate effects, one can set  $\tau_j$  in such a way that the implied marginal prior on  $\beta_j$  places substantial probability on this range. In this section, we consider the sensitivity of VC-BART's covariance effect recovery and predictive capabilities to different choices of  $\tau_j$ . Specifically, we replicate the synthetic p3R2 and p5R5 synthetic cross-sectional experiments from Section 5.1 keeping  $M = 50$  fixed but setting each  $\tau_j = \tau M^{-\frac{1}{2}}$  with  $\tau \in \{0.25, 0.5, 1, 2, 4\}$ .

Figures S1 and S2 show the average out-of-sample mean square error, frequentist coverage of the 95% uncertainty intervals, and relative uncertainty interval lengths across 50 randomly drawn training/testing splits of the data for each setting of  $\tau$ . Uncertainty interval lengths are reported relative to our recommended setting  $\tau = 1$ ; values greater than one indicate

that a particular setting of  $\tau$  results in less posterior uncertainty than  $\tau = 1$ .

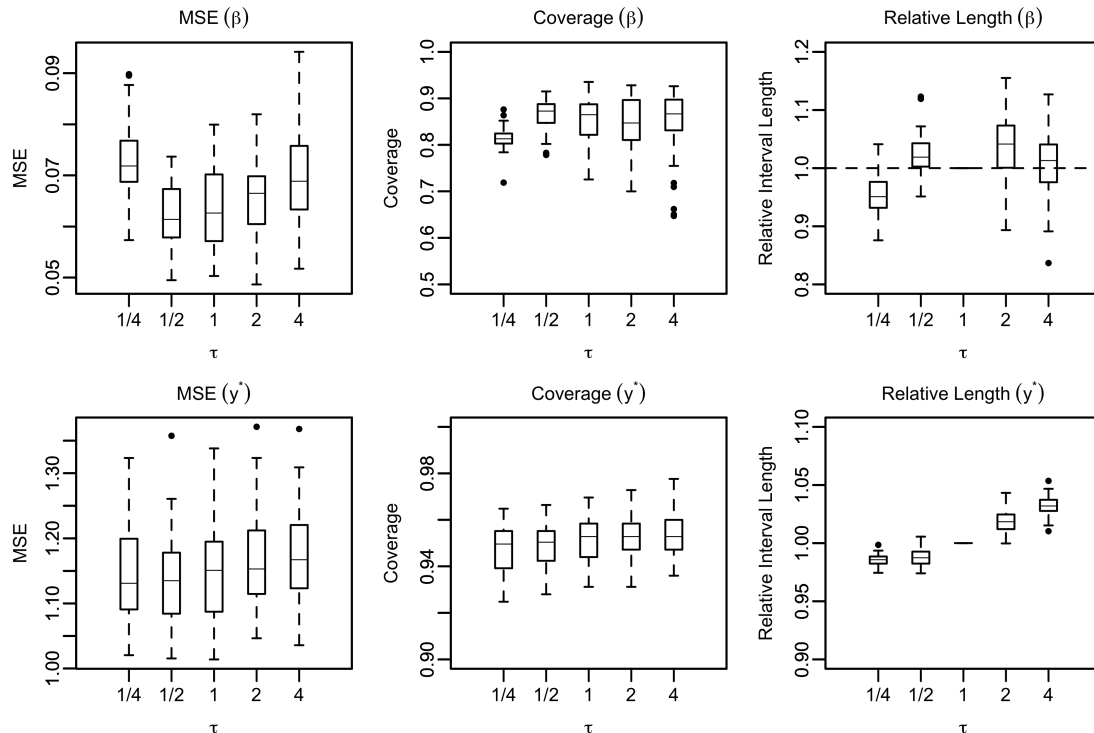


Figure S1: Sensitivity of covariate effect recovery and predictive performance across several values of  $\tau$  in the p3R2 setting.

In the p3R2 setting, we find that the overall out-of-sample MSEs for estimating covariate effects  $\beta_j(\mathbf{z})$  and new observations  $y^*$  are relatively insensitive to the choice of  $\tau$ . Similarly, the frequentist coverage of the credible intervals for  $\beta_j(\mathbf{z})$  and predictive intervals for  $y^*$  are essentially the same across the range of  $\tau$ 's considered. While it does appear that relative predictive interval lengths are increasingly monotonically in  $\tau$ , we note that the predictive intervals for  $y^*$  with  $\tau = 4$  are just about 5% larger than the intervals obtained with  $\tau = 1$ .

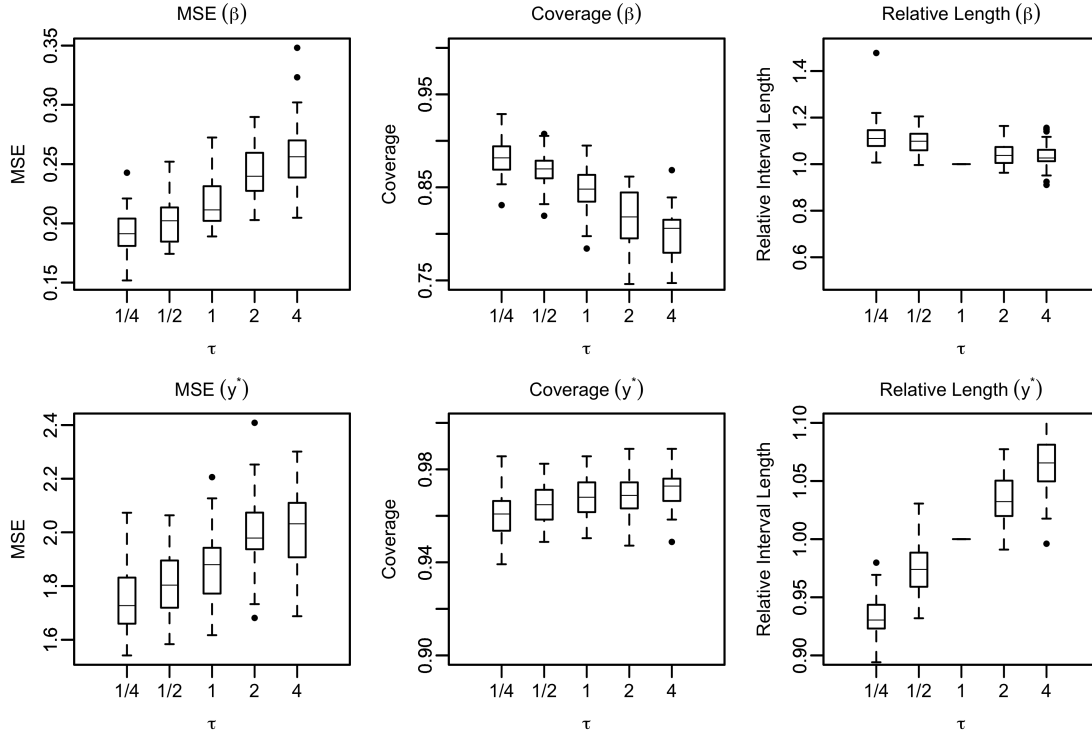


Figure S2: Sensitivity of covariate effect recovery and predictive performance across several values of  $\tau$  in the p5R5 setting.

VC-BART’s performance appears somewhat more sensitive to  $\tau$  in the p5R5 setting than in the p3R2 setting. Interestingly, as we introduce less shrinkage on the  $\beta_j(\mathbf{z})$ ’s by increasing  $\tau$ , the overall coverage of the credible intervals drops from about 87% ( $\tau = 0.25$ ) to about 78% ( $\tau = 4$ ), but the overall coverage of the predictive intervals is relatively constant. We note, however, that the range of differences in MSEs for estimating covariate effects  $\beta_j(\mathbf{z})$  and making predictions  $y^*$  is substantially smaller than the difference in MSE between VC-BART run with  $\tau = 1$  and kernel smoothing and tbVCM.

## S4 Simulation Details and Additional Results

### S4.1 Implementation and experimental details

VC-BART is implemented in C++ and interfaces with R (R Core Team, 2019) through Rcpp (Eddelbuettel and François, 2011) and RcppArmadillo Eddelbuettel and Sanderson (2014).

Our implementation uses the basic class structures of “fastBART” and tsBART (Starling et al., 2019b). We have created an R package **VCBART**, which is available online at <https://github.com/skdeshpande91/VCBART>. We performed all of the experiments reported in Sections 5 and 6 of the main text on the MIT SuperCloud high performance computing cluster. All of the experiments were run in R version 3.6.2 on nodes with 8 GB of RAM and running an Intel Xeon Gold 6248 processor.

Where possible, we ran the competing methods in our simulations with package defaults and did not implement any additional tuning procedures. For instance, the default implementation of Zhou and Hooker (2019)’s boosted tree procedure (referred to as tbVCM in Sections 5 and 6 of the main text) does not automatically perform cross-validation to set the learning rate or number of boosting iterations. Instead, in all of our experiments, we ran tbVCM for 200 iterations and with a learning rate of 0.5, which are the same settings as the example provided by the authors at <https://github.com/siriuz42/treeboostVCM>. Similarly the implementation of extremely randomized trees in the **ranger** package (Wright and Ziegler, 2017) does not automatically perform cross-validation to select the number of possible splitting variables at each node (i.e. the parameter `mtry`). In our experiments, we used the package default, setting `mtry` equal to the square root of the number of inputs.

## S4.2 Function-by-function covariate recovery performance

In the main text, we reported the covariate effect function recovery performance averaged over all  $\beta_j$ ’s in both the p3R2 and p5R5 setting. Tables 4 – 6 report the mean square error, frequentist coverage, and relative lengths of the 95% uncertainty intervals, averaged over all test set observations, for each  $\beta_j$ .

Table 4: Out-of-sample MSE of the estimated  $\beta_j$ 's in the p3R2 and p5R5 settings, averaged over 50 75%-25% training-testing splits. Standard errors are shown in parentheses. Best performance is bolded.

Method	$\beta_0$	$\beta_1$	$\beta_2$	$\beta_3$	$\beta_4$	$\beta_5$
p3R2: $n = 2500, p = 3, R = 2, \sigma = 1$						
lm	7.9 (0.2)	1.55 (0.06)	7.58 (0.35)	0.03 (0.03)		
np	0.05 (0.01)	0.14 (0.02)	0.24 (0.04)	0.12 (0.02)		
tbVCM	0.13 (0.01)	0.36 (0.03)	1.03 (0.07)	0.30 (0.03)		
VC-BART	<b>0.03</b> (0.00)	<b>0.10</b> (0.01)	<b>0.10</b> (0.02)	<b>0.02</b> (0.01)		
p5R5: $n = 2500, p = 5, R = 5, \sigma = 1$						
lm	7.92 (0.18)	1.10 (0.06)	7.38 (0.32)	0.38 (0.06)	23.21 (1.00)	0.55 (0.05)
np	1.20 (0.12)	1.11 (0.11)	1.94 (0.18)	1.37 (0.17)	3.72 (0.35)	0.84 (0.08)
tbVCM	0.58 (0.06)	0.92 (0.07)	2.13 (0.16)	1.21 (0.08)	6.65 (0.36)	0.92 (0.07)
VC-BART	<b>0.14</b> (0.04)	<b>0.24</b> (0.04)	<b>0.21</b> (0.04)	<b>0.10</b> (0.02)	<b>0.47</b> (0.05)	<b>0.14</b> (0.03)

Table 5: Out-of-sample frequentist coverage of the 95% uncertainty intervals in the p3R2 and p5R5 settings, averaged over 25 75%-25% training-testing splits. Standard errors are shown in parentheses. Best performance is bolded.

Method	$\beta_0$	$\beta_1$	$\beta_2$	$\beta_3$	$\beta_4$	$\beta_5$
p3R2: $n = 2500, p = 3, R = 2, \sigma = 1$						
lm	0.04 (0.01)	0.15 (0.02)	0.34 (0.06)	0.94 (0.24)		
np	0.93 (0.02)	0.89 (0.02)	0.92 (0.02)	0.91 (0.02)		
tbVCM	<b>1.00</b> (0.00)	<b>1.00</b> (0.00)	<b>0.93</b> (0.02)	<b>1.00</b> (0.00)		
VC-BART	0.93 (0.02)	0.84 (0.04)	0.87 (0.04)	0.79 (0.16)		
p5R5: $n = 2500, p = 5, R = 5, \sigma = 1$						
lm	0.05 (0.01)	0.34 (0.02)	0.23 (0.18)	0.63 (0.06)	0.10 (0.01)	0.45 (0.05)
np	0.71 (0.03)	0.83 (0.02)	<b>0.82</b> (0.02)	0.88 (0.02)	0.69 (0.03)	0.89 (0.01)
tbVCM	<b>1.00</b> (0.00)	<b>0.95</b> (0.01)	0.79 (0.02)	<b>0.91</b> (0.01)	0.57 (0.02)	<b>0.96</b> (0.01)
VC-BART	0.86 (0.05)	0.72 (0.07)	<b>0.82</b> (0.07)	0.87 (0.04)	<b>0.89</b> (0.02)	0.92 (0.03)

Table 6: Length of out-of-sample pointwise 95% uncertainty intervals around  $\beta_j(\mathbf{z})$  relative to VC-BART’s pointwise 95% credible intervals in the p3R2 and p5R5 settings, averaged over 25 75%–25% training–testing splits. Standard errors are shown in parentheses. Best performance is bolded.

Method	$\beta_0$	$\beta_1$	$\beta_2$	$\beta_3$	$\beta_4$	$\beta_5$
p3R2: $n = 2500, p = 3, R = 2, \sigma = 1$						
lm	<b>0.61</b> (0.02)	<b>0.62</b> (0.02)	<b>0.89</b> (0.06)	1.41 (0.16)		
np	1.30 (0.08)	1.35 (0.08)	1.95 (0.16)	3.17 (0.42)		
tbVCM	6.53 (0.25)	4.19 (0.16)	4.88 (0.34)	9.12 (1.01)		
VC-BART	1.00 (0.00)	1.00 (0.00)	1.00 (0.00)	<b>1.00</b> (0.00)		
p5R5: $n = 2500, p = 5, R = 5, \sigma = 1$						
lm	<b>0.76</b> (0.08)	<b>0.95</b> (0.08)	1.26 (0.14)	1.27 (0.11)	<b>0.54</b> (0.02)	<b>0.88</b> (0.06)
np	2.26 (0.25)	2.94 (0.25)	3.81 (0.43)	3.78 (0.36)	1.78 (0.09)	2.66 (0.21)
tbVCM	5.61 (0.58)	3.75 (0.34)	3.99 (0.43)	3.85 (0.33)	1.94 (0.08)	3.55 (0.24)
VC-BART	1.00 (0.00)	1.00 (0.00)	<b>1.00</b> (0.00)	<b>1.00</b> (0.00)	1.00 (0.00)	1.00 (0.00)